Developments in Double-Modulated Terahertz Differential Time-Domain Spectroscopy

by

Jegathisvaran Balakrishnan

B.Eng. (Electrical & Electronic, Honours),
The University of Adelaide, 2005

Thesis submitted for the degree of

Doctor of Philosophy

in

School of Electrical & Electronic Engineering,
The Faculty of Engineering, Computer, and Mathematical Sciences
The University of Adelaide, Australia

February, 2010

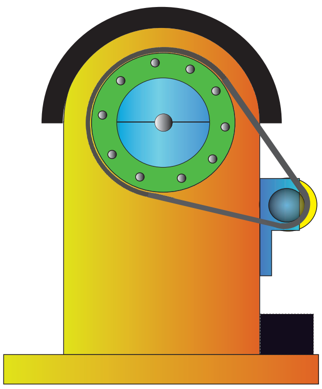

Appendix A

Modelling terahertz signal extraction using lock-in amplifier

MODELLING terahertz signal extraction using a lock-in amplifier device is explained in this chapter. The first part of the chapter gives a detailed explanation on conventional THz-TDS signal extraction using a single lock-in amplifier. The second part discusses details of double-modulated THz-DTDS signal extraction using two lock-in amplifiers. Mathematical expression and matlab simulation are included to elaborate the signal extraction techniques further for both conventional THz-TDS and double-modulated THz-DTDS.

The double-modulated THz-DTDS modelling technique described in this chapter is also used in Ch. 7 to model the rapid succesion measurement using the spinning wheel.

A.1 Terahertz signal recovery using lock-in amplifier

Recovering a very small signal in the presence of much larger background noise signal can be challenging. For example, in a T-ray spectrometer, an electro-optical or a photoconductive switching technique is employed where it often requires detection of small signals in the presence of a large noise signal. An illustration of a small signal hidden in a large noisy signal is shown in Fig. A.1. Typically, the large noise signal is composed of white noise and $1/f$ noise. It has been shown that the white noise can be reduced by simply averaging the output signals with respect to time, however this principle may not be applicable to the $1/f$ noise (Libbrecht *et al.* 2003). According to Libbrecht *et al.* (2003), the $1/f$ noise often originates from slow drifting of amplifiers and other noise generating elements over time. It has also been reported that the $1/f$ noise commonly present at very low frequencies (Dutta and Horn 1981). There are a number of ways to reduce the effect of $1/f$ noise. Conventionally, modulating the signal of interest using a mechanical chopper and recovering it using a tuned amplifier have been used widely (PerkinElmer-Instruments 2000). However, this technique is limited by the selectivity, Q factor, which may result in measurements of noise components due to a large bandwidth selection (PerkinElmer-Instruments 2000). Another approach is by using a lock-in amplifier. The lock-in amplifier allows *synchronous demodulation* or *phase sensitive detection* (PSD). The synchronous demodulation or PSD refers to a measurement of signal of interest that is synchronised in phase and frequency with the incoming reference signal. Furthermore, the lock-in amplifier is capable of providing narrowband filtering which allows an accurate measurement of the signal of interest with minimal noise interference (Stanford-Research-Systems 1999).

Traditionally, the terahertz signal generated from the conventional THz-TDS spectrometer and the double-modulated THz-DTDS spectrometer is recovered by using the lock-in amplifier. The noise present in these spectrometers is limited to not only white noise and $1/f$ noise but also other noise such as T-ray noise and laser fluctuations. In this chapter, modelling of terahertz signal extraction for a conventional THz-TDS spectrometer and a double-modulated THz-DTDS spectrometer are presented. For simplicity of the modelling, only white noise and $1/f$ noise originating from slow drifting amplifiers have been considered in this work.

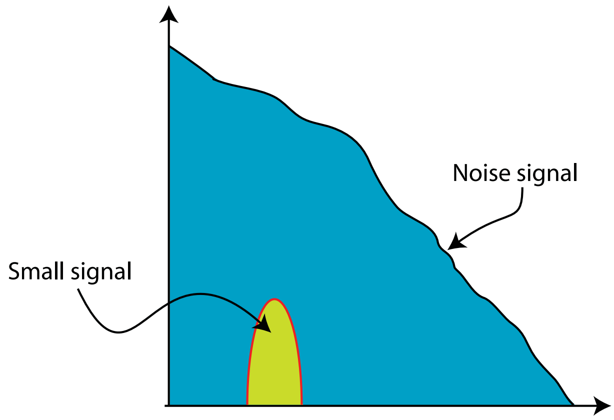

Figure A.1. Small signal hidden under a large noise signal. This figure illustrates the signal of interest hidden under a large noise signal. The noise signal is commonly originate from the white noise and the $1/f$ noise.

A.1.1 Objectives and framework

This chapter is focused on modelling the terahertz signal extraction from lock-in amplifier for terahertz time-domain spectroscopy (THz-TDS) and a double-modulated terahertz differential time-domain spectroscopy (double-modulated THz-DTDS). The modelled terahertz signal is added with white noise and $1/f$ noise for demonstration purposes. This chapter is structured as follows: In Sec. A.2, the lock-in amplifier configuration for terahertz signal extraction from a standard THz-TDS is described. In this section, a detailed description on the mathematical expression for terahertz signal recovery is given. Furthermore, a Matlab simulation for further elaboration of the concept is discussed. A lock-in amplifier configuration for double-modulated THz-DTDS is described in Sec. A.3. A detailed mathematical expression and simulation results to further elaborate the terahertz signal recovery are also discussed in this section followed by the chapter summary in Sec. A.4.

A.2 Terahertz signal extraction for a THz-TDS

In this section, modelling of the terahertz signal extraction for a conventional THz-TDS spectrometer using single lock-in amplifier is discussed. Figure A.2 shows a block diagram of a lock-in amplifier used for capturing terahertz signal. The incoming time delay dependant terahertz signal is denoted as $E(\tau_n)$ and the chopper input reference signal as $E_c(t)$.

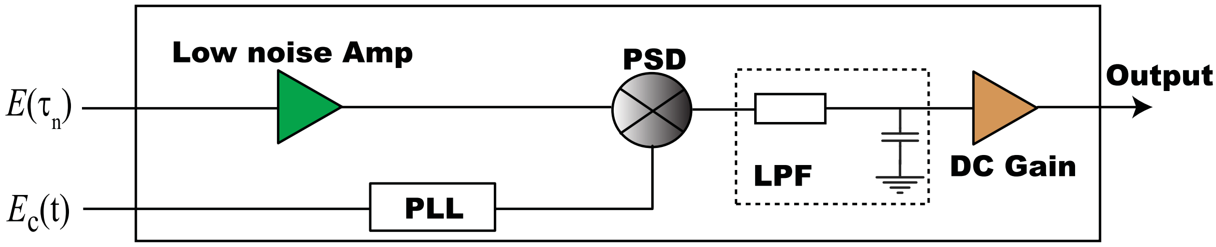

Figure A.2. Lock-in amplifier setup for conventional THz-TDS small signal recovery. This figure illustrates a block diagram of a lock-in amplifier. In a nutshell, the lock-in amplifier operates as multiplier with a narrowband filtering function.

A.2.1 Mathematical expression of the THz-TDS signal recovery using a single lock-in amplifier

Assuming that the chopper modulated terahertz signal, $E(\tau_\mathrm{n})$ is a square wave signal with an averaged amplitude, A_{τ_n} varying with the time delay, τ_n,

$$E(\tau_\mathrm{n}) = A_{\tau_\mathrm{n}}(\frac{4}{\pi}\sum_{k=1}^{\infty}\frac{\sin((2k-1)\omega_{\mathrm{chopper}}t + \phi_{\mathrm{chopper}})}{(2k-1)}) \; . \tag{A.1}$$

Here, n is the step number determined by the delay stage. The $\omega_{\mathrm{chopper}} = 2\pi f_{\mathrm{chopper}}$ represents the modulating chopper frequency. Also, the ϕ_{chopper} refers to the chopper phase. This signal is amplified at the input of the lock-in amplifier with an AC gain of G_{ac}. Thus, the amplified signal can be written as follows:

$$E_{\mathrm{ac}}(\tau_\mathrm{n}) = G_{\mathrm{ac}}E_{\tau_\mathrm{n}} \; . \tag{A.2}$$

The external chopper reference signal is obtained from a function generator that is used for modulating the optical beam. This signal is used as a reference input signal in the lock-in amplifier for signal demodulation. The external chopper reference signal can be written as follows:

$$E_\mathrm{c}(t) = V_\mathrm{f}\frac{4}{\pi}(\sum_{k=1}^{\infty}\frac{\sin((2k-1)\omega_\mathrm{c}t + \phi_\mathrm{c})}{(2k-1)}), \tag{A.3}$$

where $\omega_c = 2\pi f_\mathrm{c}$ is the reference frequency with phase, ϕ_c. Here, the chopper reference signal is phase-locked loop for synchronising the frequency and phase components with respect to the incoming terahertz signal before reaching the phase sensitive detector (PSD). The PSD act as a multiplier to produce an output signal that is a product of $E_{\mathrm{ac}}(\tau_{\mathrm{n}})$ and $E_{\mathrm{c}}(t)$,

$$E_{\mathrm{psd}}(\tau_{\mathrm{n}}) = E_{\mathrm{ac}}(\tau_{\mathrm{n}})E_{\mathrm{c}}(t) \ , \tag{A.4}$$

which can be also written as follows:

$$E_{\mathrm{psd}}(\tau_{\mathrm{n}}) = G_{\mathrm{ac}}A_{\tau_{\mathrm{n}}}V_{\mathrm{f}}\frac{4}{\pi}(\sum_{k=1}^{\infty}\frac{\sin((2k-1)\omega_{\mathrm{chopper}}t+\phi_{\mathrm{chopper}})}{(2k-1)})\frac{4}{\pi}(\sum_{k=1}^{\infty}\frac{\sin((2k-1)\omega_{\mathrm{c}}t+\phi_{\mathrm{c}})}{(2k-1)}) \ . \tag{A.5}$$

Assuming that the chopper phase, ϕ_{chopper}, is synchronised to ϕ_{c} and the chopper frequency, $\omega_{\mathrm{chopper}}$ is synchronised to ω_{c}, the modulated signal at every time delay, τ_{n} is frequency-shifted after the demodulation stage. The demodulated output is then low-pass filtered to remove the double frequency components and keep the DC component. Since the lock-in amplfier considers only the first harmonic, one may write the demodulated output as follows:

$$E_{\mathrm{psd}}(\tau_{\mathrm{n}}) = \frac{1}{2}G_{\mathrm{ac}}A_{\tau_{\mathrm{n}}}V_{\mathrm{f}}[1-\cos(2\omega_{\mathrm{chopper}}t)] \ . \tag{A.6}$$

Thus, the output signal after filtering can be written as:

$$E_{\mathrm{f}}(\tau_{\mathrm{n}}) = \frac{1}{2}G_{\mathrm{ac}}A_{\tau_{\mathrm{n}}}V_{\mathrm{f}} \ . \tag{A.7}$$

After the filtering process, the DC output can be further amplified by introducing a DC gain, G_{dc}. Thus, the time delay dependant amplified signal at the output channel of the lock-in amplifier is

$$E_{\mathrm{dc}}(\tau_{\mathrm{n}}) = \frac{1}{2}G_{\mathrm{ac}}G_{\mathrm{dc}}A_{\tau_{\mathrm{n}}}V_{\mathrm{f}} \ . \tag{A.8}$$

Figure A.3 shows a simulation results of terahertz signal extraction for a standard THz-TDS. This figure is captured at a time delay of τ_{n}.

Therefore, the sum of all dc components obtained at timing delay, τ_1 till τ_{n} produces a temporal THz pulse. This process may take several minutes depending on time constant setting of the lock-in amplifier.

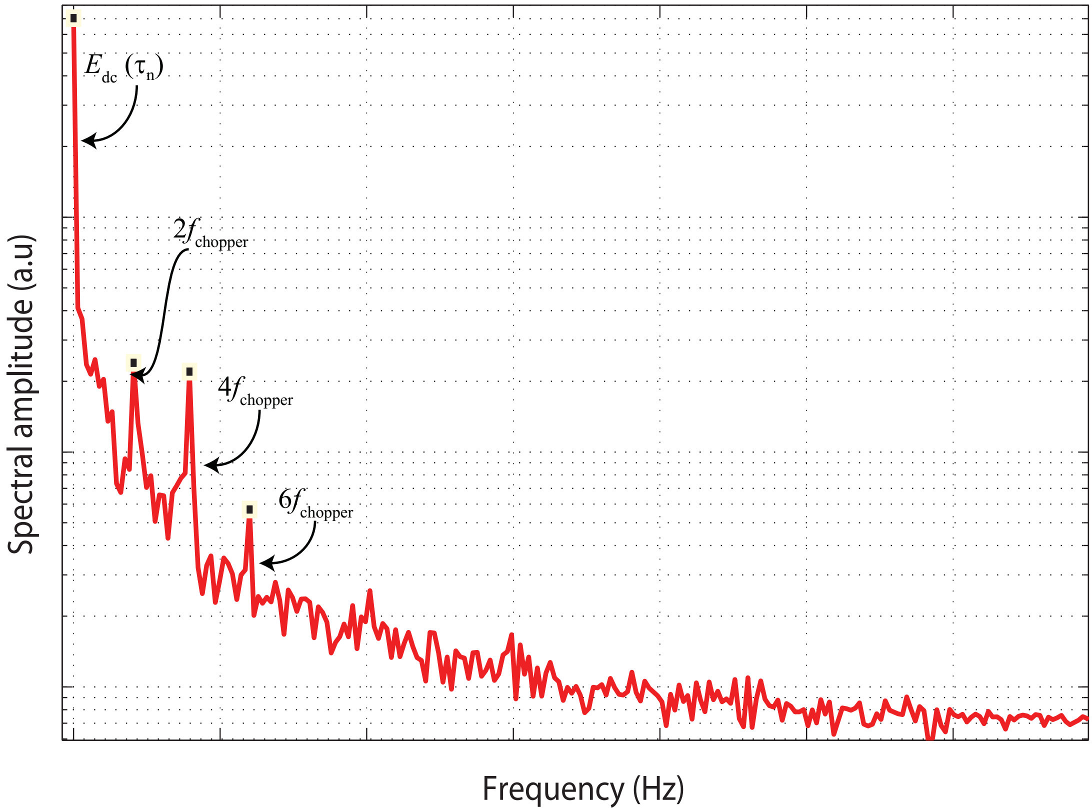

Figure A.3. Simulated terahertz signal extraction for a standard THz-TDS at the nth step of the delay stage. This figure shows the FFT of the signal detected after the demodulation and filtering stages of the lock-in amplifier. For demonstration purposes, the optical beam for generation of terahertz signal is set at f_{chopper}. The DC component, E_{dc} shown in the figure can be extracted by selecting a longer time constant. Longer time constant will result in narrower bandwidth, which means that the $2f_{\text{chopper}}$ component and above will be eliminated and only the dc component at nth step, $E_{\text{dc}}(\tau_n)$ is detected at the output channel of the lock-in amplifier.

A.3 Terahertz signal extraction for a double-modulated THz-DTDS

In the previous section, modelling of the terahertz signal using single lock-in amplifier has been discussed. By using the basic knowledge obtained from the above model, terahertz signal extraction for the double-modulated THz-DTDS is described in this section. Figure A.4 shows a block diagram of the lock-in amplifier configuration used for capturing terahertz signal from the double-modulated THz-DTDS spectrometer.

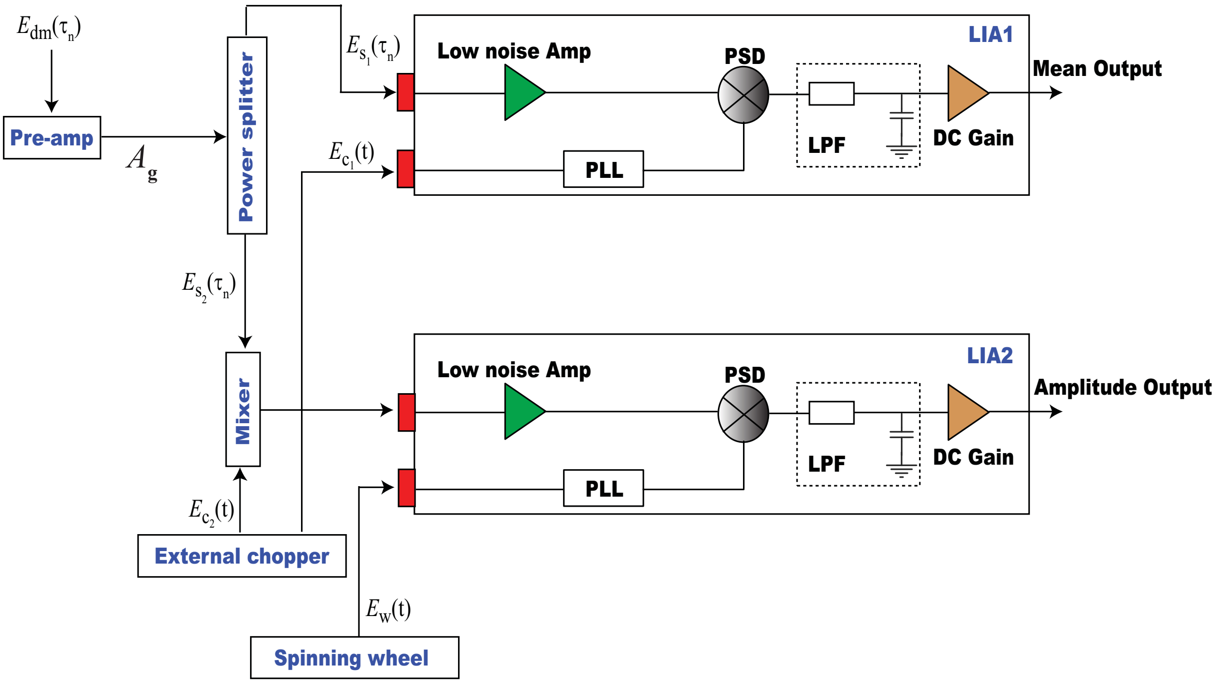

Figure A.4. Lock-in amplifier setup for double-modulated THz-DTDS small signal recovery. This figure illustrates a block diagram of dual lock-in amplifier configuration used in the double-modulated THz-DTDS spectrometer.

A.3.1 Mathematical expression of the double-modulated THz-DTDS signal recovery using two lock-in amplifiers

Assuming that the double-modulated terahertz signal, $E_{\mathrm{dm}}(\tau_{\mathrm{n}})$ is a square wave like signal, one may write the double-modulated terahertz signal as follows:

$$
\begin{aligned}
E_{\mathrm{dm}}(\tau_{\mathrm{n}}) = A_{\tau_{\mathrm{n}}}((1+\frac{4}{\pi}\sum_{k=1}^{\infty}\frac{\sin((2k-1)\omega_{\mathrm{chopper}}t+\phi_{\mathrm{chopper}})}{(2k-1)}) \\
\times(\frac{x-d}{x}(1+\frac{4}{\pi}\sum_{k=1}^{\infty}\frac{\sin((2k-1)\omega_{\mathrm{wheel}}t+\phi_{\mathrm{wheel}})}{(2k-1)})+d))\,,
\end{aligned}
\tag{A.9}
$$

where $A_{\tau_{\mathrm{n}}}$ is the averaged amplitude with varying time delay, τ_{n} and n is the step number determined by the delay stage. Here, x is the thickness of the reference sample. The sample material thickness is defined as d. Here, the $\omega_{\mathrm{chopper}} = 2\pi f_{\mathrm{chopper}}$ and $\omega_{\mathrm{wheel}} = 2\pi f_{\mathrm{wheel}}$ represent the chopper frequency and the spinning wheel frequency respectively. Also, ϕ_{chopper} refers to the chopper phase and ϕ_{wheel} refers to wheel phase. The detected double-modulated signal is further amplified using a low-noise pre-amplifier before entering the 2-way power splitter. The time delay dependant amplified signal, $E_\mathrm{p}(\tau_\mathrm{n})$ can be written as follows:

$$E_\mathrm{p}(\tau_\mathrm{n}) = A_g E_\mathrm{dm}(\tau_\mathrm{n}), \tag{A.10}$$

where A_g denotes the gain applied to the detected signal. The amplified signal is then split using a 2-way power splitter to produce the split signals, $E_{\mathrm{s}_1}(\tau_\mathrm{n})$ and $E_{\mathrm{s}_2}(\tau_\mathrm{n})$. These signals enter the input channel of the lock-in amplifier one (LIA1) and the input channel, $X_\mathrm{modulator}$ of the mixer respectively. The $E_{\mathrm{s}_1}(\tau_\mathrm{n})$ and $E_{\mathrm{s}_2}(\tau_\mathrm{n})$ are described as follows:

$$E_{\mathrm{s}_1}(\tau_\mathrm{n}) = E_{\mathrm{s}_2}(\tau_\mathrm{n}) = \frac{1}{2}E_\mathrm{p}(\tau_\mathrm{n}). \tag{A.11}$$

An AC gain applied at the input of the LIA1:

$$E_{\mathrm{ac}_1}(\tau_\mathrm{n}) = G_{\mathrm{ac}_1} E_{\mathrm{s}_1}(\tau_\mathrm{n}) \ . \tag{A.12}$$

According to the lock-in amplifier configuration shown in Fig. A.4, an external chopper reference frequency is required for demodulation process at the LIA1 and the mixer. The chopper reference frequency is generally obtained from the frequency generator used for modulating the optical beam path discussed in Ch. 3. In this configuration, a splitter is used to split the incoming chopper frequency before entering the input reference channel of the LIA1 and the X_carrier input reference channel of the mixer. The external reference signal can be written as follows:

$$E_{\mathrm{c}_1}(t) = E_{\mathrm{c}_2}(t) = \frac{1}{2}(1 + V_\mathrm{c}\frac{4}{\pi}(\sum_{k=1}^{\infty}\frac{\sin((2k-1)\omega_\mathrm{c}t + \phi_\mathrm{c})}{(2k-1)})), \tag{A.13}$$

Here, $\omega_c = 2\pi f_\mathrm{c}$ is the reference frequency with phase, ϕ_c. The phase sensitive detector (PSD) of LIA1 produces an output signal that is a product of $E_{\mathrm{ac}_1}(\tau_\mathrm{n})$ and $E_{\mathrm{c}_1}(t)$. This stage is also known as demodulation stage. Hence, the PSD output of LIA1 is

$$E_{\mathrm{psd}_1}(\tau_\mathrm{n}) = E_{\mathrm{ac}_1}(\tau_\mathrm{n})E_{\mathrm{c}_1}(t) \ . \tag{A.14}$$

Assuming that the chopper phase, ϕ_{chopper}, is synchronised to ϕ_{c} and the chopper frequency, $\omega_{\mathrm{chopper}}$ is synchronised to ω_{c}, the double-modulated signal is frequency-shifted after the demodulation stage. The demodulated output is then low-pass filtered to remove the redundant information and only DC component will be taken into account for DC amplification. Thus, the output signal detected at LIA1 is denoted as the time delay dependant mean signal, $E_{\mathrm{mean}}(\tau_{\mathrm{n}})$.

On the other hand, the $E_{\mathrm{s}_2}(\tau_{\mathrm{n}})$ entering the $X_{\mathrm{modulator}}$ input channel of the mixer is multiplied with the $E_{\mathrm{c}_2}(t)$. The mixer is designed without filtering effect so that better accuracy on the signal extraction at the LIA2 can be obtained as compared to the previously presented works (Mickan *et al.* 2002b, Mickan *et al.* 2004, Balakrishnan *et al.* 2006, Balakrishnan *et al.* 2008). The product of the mixer is then fed into the input channel of the LIA2. The product of the mixer can be written as follows:

$$P_{\mathrm{out}}(\tau_{\mathrm{n}}) = kE_{\mathrm{s}_2}(\tau_{\mathrm{n}})E_{\mathrm{c}_2}(t) \,, \tag{A.15}$$

where k is the scaling factor. The mixer output signal obtained at the τ_{n} is illustrated in Fig. A.5. According to the lock-in amplifier configuration shown in Fig. A.4, the $P_{\mathrm{out}}(\tau_{\mathrm{n}})$ serves as an input signal to LIA2.

Here, as the LIA2 receives incoming signal from the mixer, an AC gain is applied for amplification,

$$E_{\mathrm{ac}_2}(\tau_{\mathrm{n}}) = G_{\mathrm{ac}_2}P_{\mathrm{out}}(\tau_{\mathrm{n}}) \,. \tag{A.16}$$

For demodulation purposes, an external reference signal, f_{w} is obtained from the spinning wheel device (described in Ch. 7 and 8) that is used for modulating the terahertz beam. This signal is used as a reference input signal in the lock-in amplifier for signal demodulation. The external reference signal generated by the spinning wheel can be written as follows:

$$E_{\mathrm{w}}(t) = 1 + V_{\mathrm{w}}\frac{4}{\pi}\Big(\sum_{k=1}^{\infty}\frac{\sin((2k-1)\omega_{\mathrm{w}}t + \phi_{\mathrm{w}})}{(2k-1)}\Big). \tag{A.17}$$

Here, $\omega_{\mathrm{w}} = 2\pi f_{\mathrm{w}}$ is the spinning reference frequency with phase, ϕ_{w}. The PSD of LIA2 produces an output signal that is a product of $E_{\mathrm{ac}_2}(\tau_{\mathrm{n}})$ and $E_{\mathrm{w}}(t)$. Hence, the PSD output is

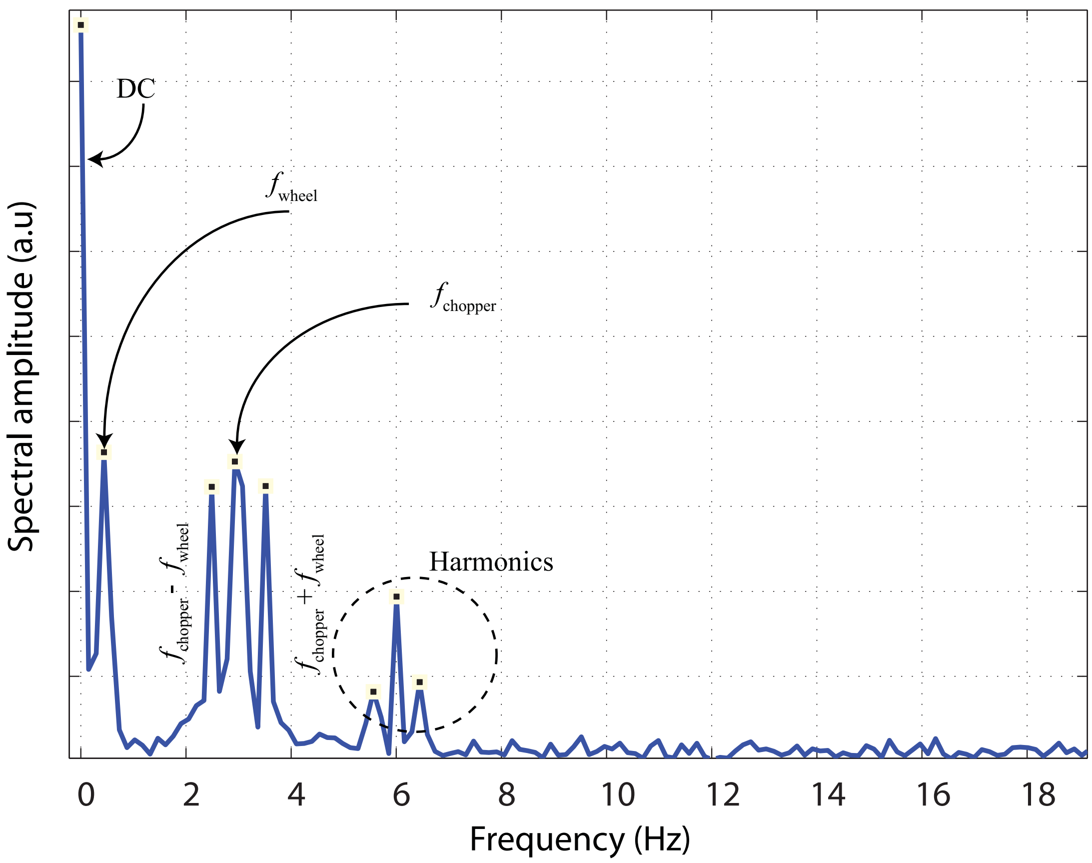

Figure A.5. Simulated mixer output at nth step of the delay stage in frequency domain. This figure illustrates the product of $X_{\mathrm{modulator}}$ and X_{carrier} channels of the mixer at the nth step of the delay stage in frequency domain. The $X_{\mathrm{modulator}}$ input channel is fed with the simulated double-modulated signal, $E_{\mathrm{s}_2}(\tau_{\mathrm{n}})$ with f_{chopper} of 3 Hz and f_{wheel} of 0.5 Hz and the X_{carrier} input channel is fed with the simulated chopper reference signal, $E_{\mathrm{c}_2}(t)$ with f_{c} of 3 Hz. Thus, the simulated $E_{\mathrm{s}_2}(\tau_{\mathrm{n}})$ consists of a sum component (3 Hz + 0.5 Hz) and a difference component (3 Hz - 0.5 Hz) as illustrated in the figure above. With the assumption that the phase and frequency components of $E_{\mathrm{s}_2}(\tau_{\mathrm{n}})$ synchronises to the phase and frequency components of $E_{\mathrm{c}_2}(t)$, one can deduce the output of the mixer, $P_{\mathrm{out}}(\tau_{\mathrm{n}})$ as shown in the figure. Therefore, the simulated double-modulated signal will be shifted towards the DC at the output of the mixer. The shifted components will then enter the input channel of LIA2 for further demodulation process to produce the amplitude signal.

$$E_{\mathrm{psd}_2}(\tau_\mathrm{n}) = E_{\mathrm{ac}_2}(\tau_\mathrm{n}) E_\mathrm{w}(t) \; . \tag{A.18}$$

Assuming that the wheel's phase, ϕ_wheel, is synchronised to ϕ_w and the wheel frequency, ω_wheel is synchronised to ω_w, the amplified signal is further frequency-shifted after the PSD stage. This signal is then low-pass filtered to remove the redundant information and only DC component will be taken into account for DC amplification. Thus, the output signal detected at LIA2 is known as the time delay dependant amplitude signal, $E_\mathrm{amplitude}(\tau_\mathrm{n})$.

According to (Mickan *et al.* 2004, Mickan 2003), with the above mean and amplitude signals, one may extract the reference and sample signals according to the following formula:

$$\widetilde{E}_\mathrm{reference}(\tau_\mathrm{n}) = \widetilde{E}_\mathrm{mean}(\tau_\mathrm{n}) + \widetilde{E}_\mathrm{amplitude}(\tau_\mathrm{n}) \; , \tag{A.19}$$

$$\tilde{E}_\mathrm{sample}(\tau_\mathrm{n}) = \widetilde{E}_\mathrm{mean}(\tau_\mathrm{n}) - \widetilde{E}_\mathrm{amplitude}(\tau_\mathrm{n}) \; . \tag{A.20}$$

A.4 Chapter summary

This chapter has described a modelling technique for terahertz signal extraction using the lock-in amplifier. In Sec. A.2, a detailed modelling technique for a standard THz-TDS has been presented. Section A.3 described a detailed modelling technique for double-modulated THz-DTDS. In these modelling work, white noise and $1/f$ noise originating from the slow drifting amplifiers have been considered for demonstration purposes. The modelling techniques presented in this chapter are used extensively in Ch. 7 to model the rapid succession measurement using the spinning wheel.

Appendix B

Terahertz detection of substances

T-RAYS have proven to be of great use in the detection of biological and nonmetallic substances that are not readily detected by other means. In many instances, conventional methods of retection (detection of hidden objects or substances within a package), such as X-rays manage only to reveal dense objects, but have difficulties in detecting plastic objects or soft biological materials. T-rays are able to improve on X-rays, due to their ability to detect nonmetallic and nonploar substances, as well as offering spectroscopy of these substances.

This chapter will look into the use of transmission mode technique to detect various illicit substances in a suitcase. Common materials used in bags and suitcases such as nylon, polycarbonate, and polyethylene are used to sandwich various illicit substances and are scanned by the commercially available Picometrix™ T-Ray 2000 system to obtain spectral data, simulating the probing of a suitcase.

B.1 Introduction

With the current global security standards being constantly upgraded, a method in which to rapidly and non-invasively scan bag and package contents is an ever growing concern. As current imaging techniques have difficulty in scanning and identifying non-metal and biological substances that could be hidden within a bag or a packages, the need for detection of these potential hazards becomes increasingly important. Terahertz time-domain spectroscopy (THz-TDS) can provide an efficient method of detecting the substances under test. Biological substances, explosives and narcotics have already been proven to show a distinctive spectral signature under THz-TDS (Wang *et al.* 2003, Fischer *et al.* 2005a, Federici *et al.* 2005, Shen *et al.* 2005, Te *et al.* 2002, Kawase *et al.* 2003), however work is still required to ensure these signatures can be detected within a concealed bag or package, which is explored in this chapter.

B.1.1 Objectives and framework

The work that this chapter aims to express is a proof-of-concept in the use of THz-TDS in secure areas, such as airports, postal agencies and shipping ports to accurately and efficiently identify substances that are hidden inside bags and packages brought into these areas. This is achieved by a number of steps. Firstly, THz spectra of materials found in bags, (for example, plastics and cotton) must be recorded. Then, after the bag or package is scanned, an algorithm along with the previously recorded reference data interrogates the spectral content of the bag or package to determine the contents. For illicit substances the algorithm then flags the bag or package, displays the type of illicit substance detected, and notifies the operator immediately to take action. This chapter is structured as follows: The methodology involved in simulating a suitcase and contents is described is described in Sec. B.2. A brief description on the Picometrix^{TM} T-ray 2000 experimental setup used in this measurement is given in Sec. B.3. The results and discussion are elaborated in Sec. B.4 followed by conclusion and recommendation in Sec. B.5.

B.2 Methodology

Initially, spectral data from common packing materials are examined for transparency under THz, following which the THz spectrum of the materials are collected. Plastics that are used in common backpacks or suitcases are investigated and tested for transparency and their respective THz spectrum are recorded. Cotton is also tested for transparency to simulate clothing and its THz spectrum is also recorded. The THz spectrum of a given substance can then be recorded for use in an algorithm for detection.

From a cross-sectional angle, bags and suitcases can be viewed as two plastic sheets forming the outer layers, while the contents (for this work, simple clothing) can be simulated by a cotton sheet. This then forms the basis for the simulation of a suitcase and contents (Fig. B.1). A substance can then be laced onto the cotton, and its signature can be recovered if the data from a clean simulation sample is subtracted from the laced sample data. A specialised sample holder is designed and implemented to carefully hold the sample in place and ensure the air gap between the various materials is kept to a minimum. This involves clamping the materials together as tightly as possible. The thickness of the samples is variable, while the width and length of each sample remains as a 50 mm square.

NOTE:
This figure is included on page 147 of the print copy of the thesis held in the University of Adelaide Library.

Figure B.1. Simulation of a faux suitcase and contents. The faux suitcase showing two plastic outer layers, with cotton sandwiched between, and laced with a substance. Note that the spiral indicates the laced substance. After Ung *et al.* (2006).

B.3 Experimental Setup

The Picometrix™ T-ray 2000 system is shown in Fig. B.2. A Maitai Ti-sapphire femtosecond modelocked laser is used as a source of optical pulses. This laser provides 210 nm (710 - 920 nm) in useable tuning range with over 2.5 W of average power and a pulse width of less than 100 fs at a repeatition rate of 80 MHz. Both the THz transmitter and detector utilize Bowtie photoconductive antennas. The sample, along with

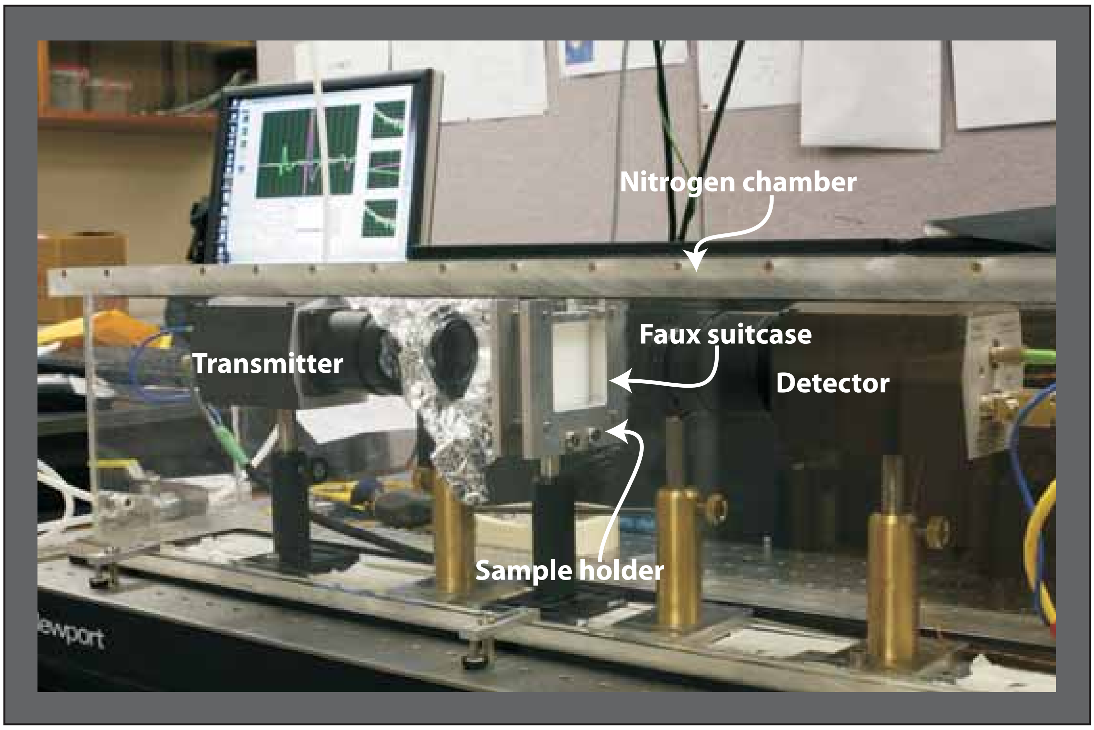

Figure B.2. Picometrix™ T-Ray 2000 spectrometer. This schematic diagram shows a typical Picometrix™ T-Ray 2000 spectrometer. The sample under test is placed at the focal plane.

the transmit and detect heads, is placed within a semi-airtight nitrogen chamber. The chamber is then purged with pure nitrogen to remove water vapour. The purging minimises water lines from appearing in the measured spectrum. This measurement is conducted at room temperature. To ensure the plastics and cotton fit onto the metal sample holder and be pressed together to minimise air gaps, the sheets are cut into 50 mm square pieces with 2 holes drilled into each corner. Two plastic sheets are needed for each sample. The lacing of the cotton is carried out with small amount of α-lactose monohydrate (Sigma-Aldrich Co.), which is mixed into a solution of water and poured over the cotton sheet to create an even layer of lactose across the cotton. The cotton is then left to dry after which it is placed in between the plastic sheets.

B.4 Results and discussion

In a proof-of-concept experiment, it is shown that T-rays are able to penetrate various common plastics and detect a trace substance laced on a piece of cotton wedged between them. The experiment uses α-lactose, which has distinct terahertz absorption peaks at approximately 0.52 and 1.38 THz (Fig. B.3a). The experiment shows that when a small amount of lactose is laced onto cotton fabric, and then sandwiched between two sheets of the same plastic, the absorption peaks are still readily detectable (Fig. B.3b, red plot). This is opposed to similar lactose-free setup, where no absorption peaks are seen (Fig. A.3b, blue plot).

Two plastic sheets surrounding the cotton appear only to attenuate the absorption peaks and add interface reflection noise as shown in Fig. B.3a and Fig. B.3b. This shows that other organic and non-metal substances may be detectable under similar circumstances.

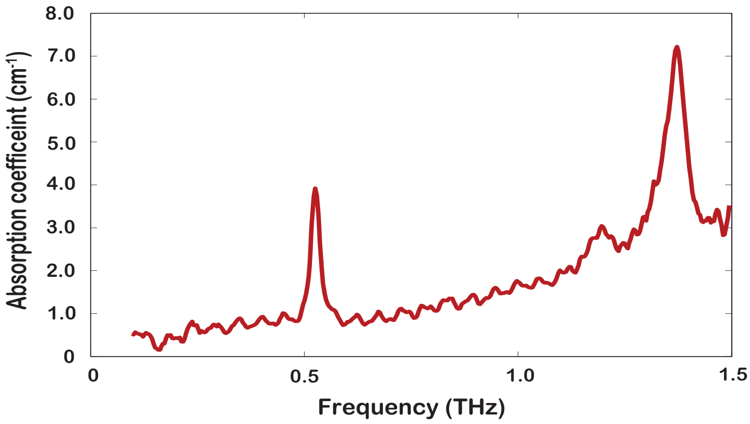

(a)

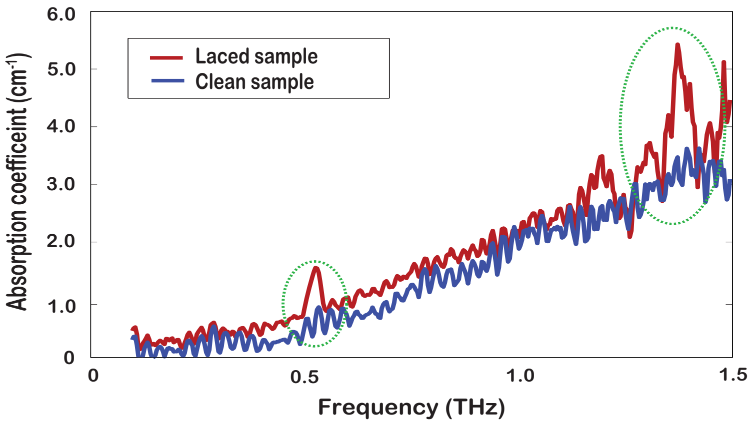

(b)

Figure B.3. Absorption curves of α-lactose, clean and laced samples of the faux suitcase. (a) T-ray absorption spectrum of α-lactose monohydrate at room temperature from 0.1 to 1.5 THz. Distinct peaks can be seen at approximately 0.52 and 1.38 THz, which are unique to α-lactose, showing its distinct T-ray signature. In comparison, (b) shows the T-ray spectrum of a nylon cotton sandwich, with both a clean sample (blue plot) and an α-lactose laced sample (red plot) at room temperature. Two sheets of nylon, each with a thickness of 3.205 mm, were pressed together with a sheet of cotton (0.442 mm thick) in between in order to crudely simulate the profile of a plastic suitcase. The resultant spectra for clean sample shows no signature absorption peaks. Absorption of the T-ray signal is increased with increasing frequencies, as the nylon and cotton absorb the signal to a greater degree. Signal noise and interface reflections can also be seen in the data. The laced sample clearly shows the signature absorption peaks from (a) when the cotton is laced with α-lactose. The circled areas clearly show the absorption peaks at approximately 0.52 and 1.38 THz, which are characteristic to α-lactose, indicating that it is present in this particular sample. After Ung *et al.* (2006).

B.5 Conclusion and recommendation

From these experiments, a proof-of-concept of the use of THz-TDS in secure areas, for the screening and detection of illicit substances in bags and packages, is achievable provided that a library containing spectral signatures of many substances is available and a suitable and accurate algorithm to determine the substances is present. For future work, higher bandwidth T-ray signals would also aid the detection and identification of illicit substances, as this would provide a larger set of unique features due to the wider frequency range. Deeper penetration of bags and packages would also be required, thus greater signal power is needed. If this can be achieved, the possibility of bringing such a machine into reality and use in secure areas is possible.

Appendix C

Experimental Equipment

THE equipment used in the conventional THz-TDS and double-modulated THz-DTDS measurements are described in further detail in this appendix. Data acquisition techniques using LabVIEW™ are discussed in this appendix. The signal analysis technique using MATLAB is covered in Appendix D.

C.1 Conventional THz time-domain spectrometer

Figure C.1 shows the layout of the conventional THz time-domain spectrometer used in our lab. Most of the experimental results presented in this Thesis are obtained from this spectrometer. This section describes the equipment used for implementing the conventional terahertz time-domain spectrometer. The laser system, optical and mechanical components are attached to a vibration proof optical table. Other components such as lock-in amplifier and motion controller are placed under the optical table to avoid tripping. Also, a custom-built nitrogen chamber is attached to the optical table as shown in the figure. This chamber is purged with nitrogen during measurements to minimise the water lines effect.

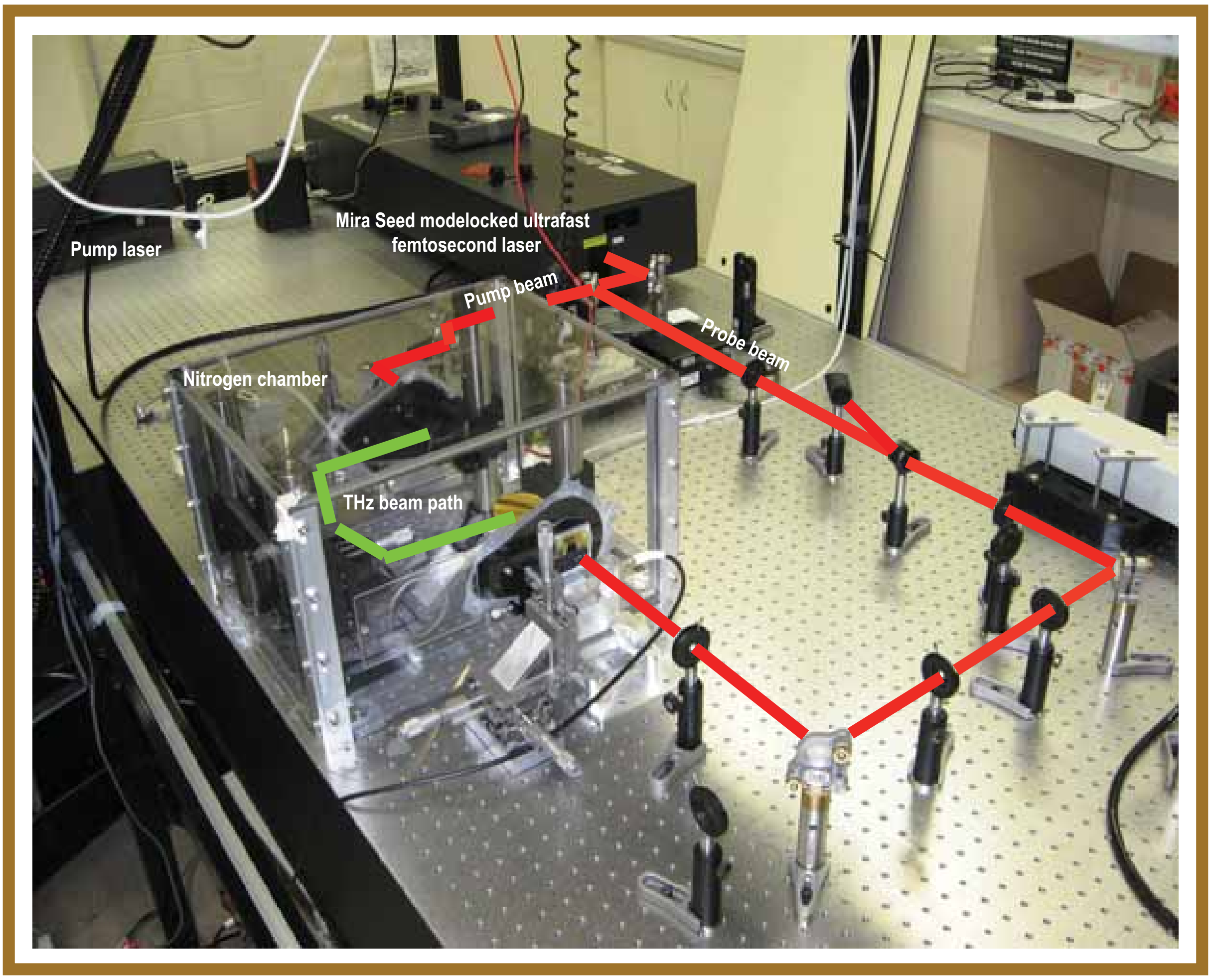

Figure C.1. Conventional terahertz time-domain spectrometer. This figure shows the T-ray spectrometer used for measurements in this thesis. The components used to build this spectrometer are described in the text.

C.1.1 Modelocked femtosecond laser

The laser system used in the above spectrometer for generation and detection of terahertz radiation is known as MiraSeed modelocked ultrafast laser manufactured by Coherent, Inc. (Fig. C.2). This laser uses Titanium: sapphire crystal to produce ultrashort, wide bandwidth, and femtosecond pulses. This laser is used to produce the pump and probe beams to generate and detect terahertz radiation.

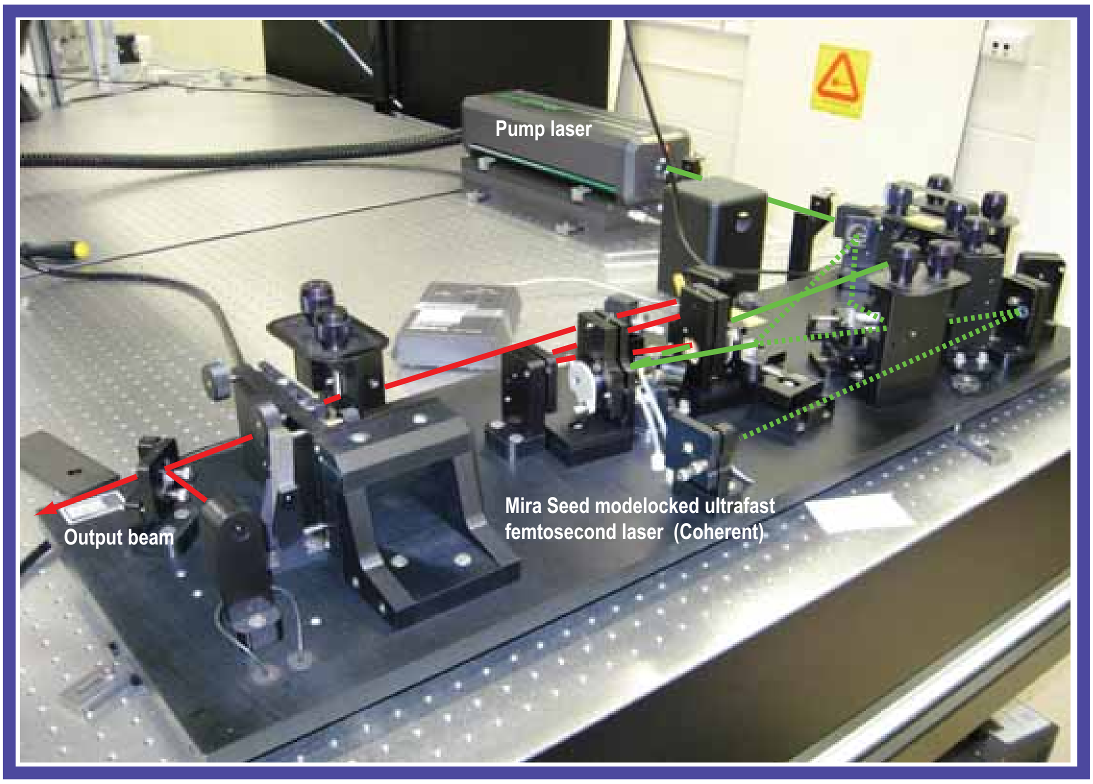

Figure C.2. A MiraSeed Ti-sapphire femtosecond modelocked laser. This photograph shows the interior of Mira Seed modelocked ultrafast femtosecond laser that is used as a source of optical pulses. The Seed is pumped by Verdi V6 laser with a wavelength of 532 nm. The femtosecond laser produces an output pulse duration of 20 fs at a repetition rate of 76 MHz. This laser has an output power of 1 W with a centered wavelength at 800 nm.

C.1.2 XPS Motion controller

Figure C.3 shows a XPS motion controller and a motorised delay stage manufactured by Newport Corporation. These devices are used for gating the THz signal generated through the spectrometer. The motion controller allows high-speed communication through 10/100 Base-T Ethernet and capable of controlling up to 8 axes (i.e., motorised delay stages) concurrently.

(a) XPS Motion Controller

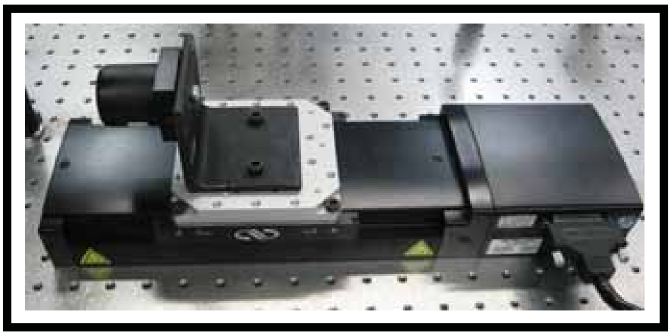

(b) Motorised delay stage

Figure C.3. XPS motion contoller and motorised delay stage. This figure depicts the XPS contoller used for delaying the motorised delay stage at the pump beam of the T-ray spectrometer. This controller is capable of handling of up to 8 channels and allows high-speed communication through 10/100 Base-T Ethernet connection. Further details can be found in the manufacturer's manual.

C.1.3 Lock-in amplifier configuration

A photograph of a standard Stanford Research System SR830 lock-in amplifier (LIA) used in the T-ray spectrometer is shown in Fig. C.4. The full operational details of LIA model SR830 can be found from the manufacturer's manual. In a nutshell, the SR830 LIA is used to demodulate the incoming terahertz signal from the detector with an appropriate reference signal. There are two main parts to the operation of this lock-in amplifier: first, the demodulation process at a Phase Sensitive Detector (PSD) and second, filtering at a narrow band low pass filter (LPF). In a conventional terahertz time domain spectrometer, the lock-in amplifier uptakes two input signals; an input signal (terahertz signal) and a reference signal (chopper signal). These signals are then multiplied to produce sum ($2f$) and difference components (DC). With an assumption that both the input and reference signals are synchronised in both frequency and phase, the narrowband low pass filter will attempt to filter any frequency component above the DC. The SR830 allows narrow bandwidth selection and this can be achieved by increasing the time constant. According to the manufacturer's manual, the relationship between the filter bandwidth and the LIA time constant can be written as follows:

$$\mathrm{BW}_{\mathrm{LIA}} = \frac{1}{S \times T} \tag{C.1}$$

where T represents the lock-in amplifier's time constant and S refers to the slope of the filter. This lock-in amplifier allows slope settings of 6 db/octave, 12 db/octace, 18 db/octave, and 24 db/octave. Therefore, the dc output obtained at the output channel of the LIA is transfered to the computer for signal capturing and data analysis. The principles of operation of lock-in amplifier in demodulating the terahertz signal is described through simulation technique in Appendix. A.

Figure C.4. Photograph of SR830 lock-in amplifier. This figure shows the photograph of the SR830 model lock-in amplifier.

C.1.4 SR540 chopper controller

Figure C.5 depicts the SR540 chopper controller and the chopper device used for modulating the optical beam and also as an external reference signal to the lock-in amplifier. The controller shown in Fig. C.5a allows chopping frequency of up to 4 kHz. Figure C.5b shows the chopper wheel used to interrupt the optical beam. The chopper wheel is equally spaced to provide 50% duty cycle. The chopper wheel is placed at pump beam of the spectrometer.

(a) SR540 Chopper controller

(b) Chopper wheel

Figure C.5. SR540 Chopper system. This figure illustrates the SR540 chopper system composed of a chopper controller and a chopper wheel. This system is capable of handling chooping frequency of up to 4 kHz.

C.1.5 Optical components

This section describes the optical components used in the terahertz setup described in Chapter 3. These components are commercially available from standard optics suppliers (i.e., Newport Corp., Thorlabs).

Mirrors and lens

A number of pyrex mirrors with high surface quality and broadband coating for the ultrafast 800 nm pulses are used. These mirrors are mainly used for reflecting the laser beam. These mirrors are 25.4 mm in diameter that is sufficiently wide to handle the optical beam size. Since the photoconductive antennas used in the spectrometer operate at low power, neutral density (ND) filters are required to filter the laser output power. Optical lenses are also used in our terahertz setup. These lenses are used for focusing the optical beam into the photoconductive antennas to generate THz pulse. Moreover, a gold-plated retroreflector mounted on a delay stage is used to adjust the path length. A 50:50 antireflection beam splitter for splitting the laser pulses into pump and probe beams is also used in our setup. Gold-coated parabolic mirrors are used for collimating and focusing T-rays.

C.1.6 Mechanical components

The XYZ stages and the custom-built photoconductive antenna mounts are considered to be the mechanical components for the terahertz spectrometer apart from the motorised delay stage and the optical chopper wheel described in the above sections. The function of the XYZ stage is to hold the optical lens and adjust in the XYZ direction. The XYZ stage plays an important role in optimising the system's bandwidth.

The custom-built photoconductive antenna mounts are depicted in Fig. 3.9. These mounts are specially designed to hold the photoconductive antennas described in Ch. 3. The main body of the mount is made from aluminium. According to Fig. 3.9, the photoconductive antenna is placed on the antenna slider that moves in a single direction. For coupling and collimation purposes, a Si hyperhemispherical lens is attached to the back of the photoconductive antenna as shown in the Fig. 3.9. Here, a custom-made finger mounted on a XY stage is used to hold the Si hyperhemispherical lens.

C.2 Data acquisition for conventional THz-TDS

The THz-TDS spectrometer described in this Thesis is controlled by using a graphical tool called LabVIEW^{TM} version 8.5. This tool is mainly used for controlling the motion controller that moves the delay stage and collects the terahertz signal from the lock-in amplifier. Here, in order to achieve high speed communication, the motion controller is connected to the computer terminal through 10/100 Base-T Ethernet. On the other hand, a General Purpose Interface Bus (GPIB) card and a GPIB cable are required for establishing communication between the lock-in amplifier and the computer terminal. Figure C.6 shows a screen shot of a LabVIEW program for a THz-TDS transmission spectrometer. This program was originally written by Matthias Hoffmann from the University of Freiburg, however, a slight modification has been made to meet the desired functionality.

Features of this program are as follows:

- Input parameter - Users can insert desired parameters such as number of steps, step size, and number of scans.
- File name labelling and browsing.
- Lock-in parameter - Users can set the sensitivity, time constant, GPIB address, and input configuration.
- Time - The expected time to finish the scan.
- View of live temporal shape, spectral amplitude, and saved spectra.
- Automatic save to disk function

The program plots the temporal profile and saves it for analysis. The analysis is carried out using Matlab software program described in the Apppendix D (see Sec. D.1).

C.3 Double-modulated THz-DTDS spectrometer

The double-modulated THz-DTDS is implemented based on the conventional THz-TDS without modification on the hardware. However, slight change in the method of signal extraction and data aquisition is required. In this section, the equipment used and the method of signal extraction are described.

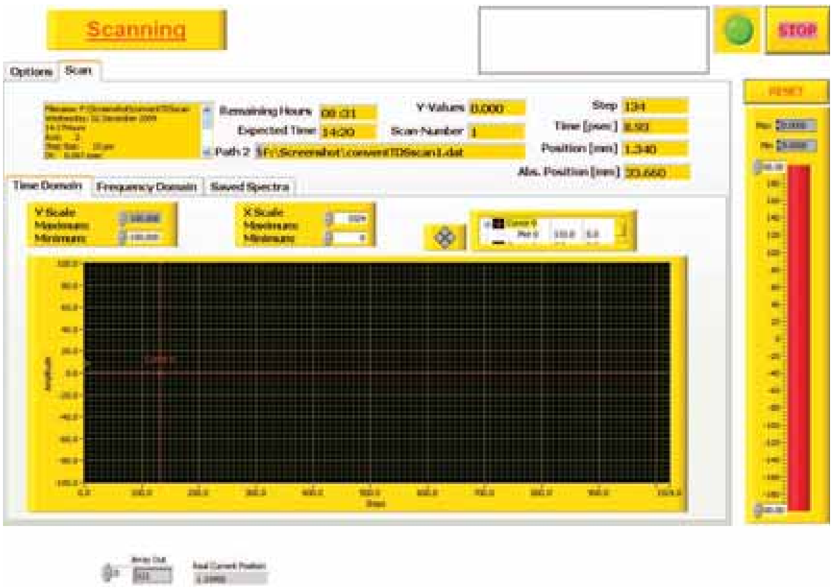

Figure C.6. Screen shot of the LabVIEW program for conventional THz-TDS spectrometer. This program was developed to control the motion controller and acquired terahertz data from the lock-in amplifier. The 'Options' tab is used to insert parameters to control the motion controller and the lock-in amplifier (not shown in the figure). A live view of the temporal profile, spectral amplitude, and saved spectra can be attained from the graph indicator shown above.

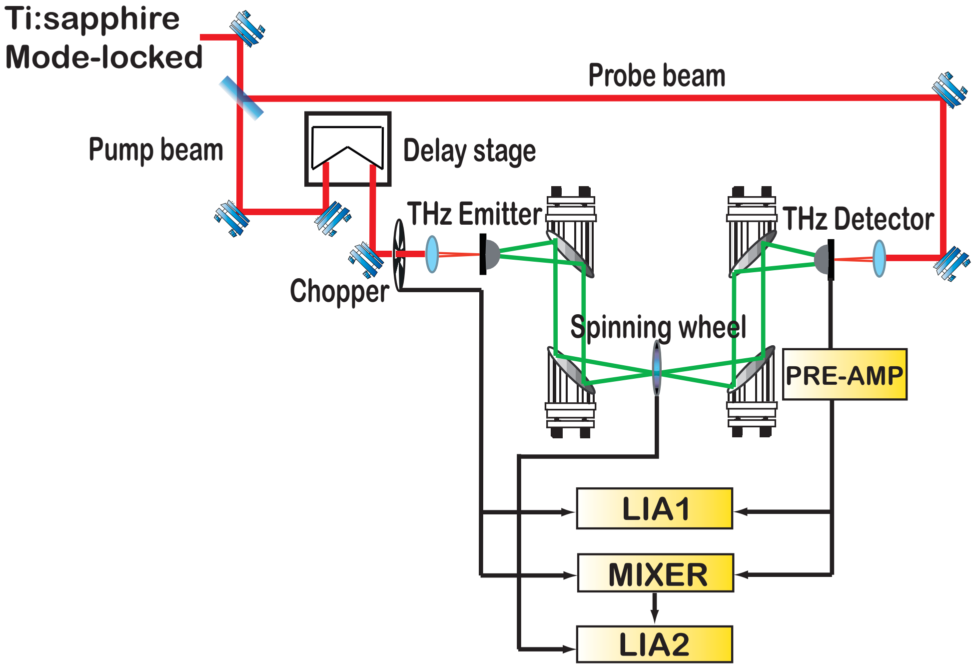

Figure C.7. Double-modulated THz-DTDS spectrometer. This figure shows the schematic diagram of the double-modulated THz-DTDS spectrometer. The spectrometer is widely used for measurements of polymer materials and liquids presented in Ch. 7 and Ch. 8. The incoming femtosecond laser is split into pump and probe beam using a beam splitter which will then go through optics for generating and detecting the THz signal. The spinning wheel is placed in the THz beam and modulated at certain speed.

C.3.1 Double-modulated THz-DTDS

Figure C.7 illustrates the double-modulated THz-DTDS schematic diagram. In a conventional THz-TDS two separate mechanical delay scans are required to obtain the reference and sample pulses, however, in this technique, only one mechanical delay scan is required for obtaining the reference and sample pulses. This can be achieved by introducing the spinning wheel device and dual lock-in amplifier configuration.

C.3.2 Dual lock-in amplifier configuration

The double-modulated signal obtained from the above spectrometer is fed into the lock-in amplifier configuration shown in Fig. C.8. This configuration consists of a SR560 preamplifier, two power splitters, a custom-built mixer, and two SR830 lock-in amplifiers. The preamplifier is used to scale the output level from the THz detector to ensure that the signal entering the lock-in amplifiers is detectable. The power splitters are used to split the amplified double-modulated signal and the chopper frequency while the mixer is used for demodulating the double-modulated signal at a chopper reference frequency. Here, the mixer is designed without a filter. The lock-in amplifiers are used to extract the mean and amplitude signals.

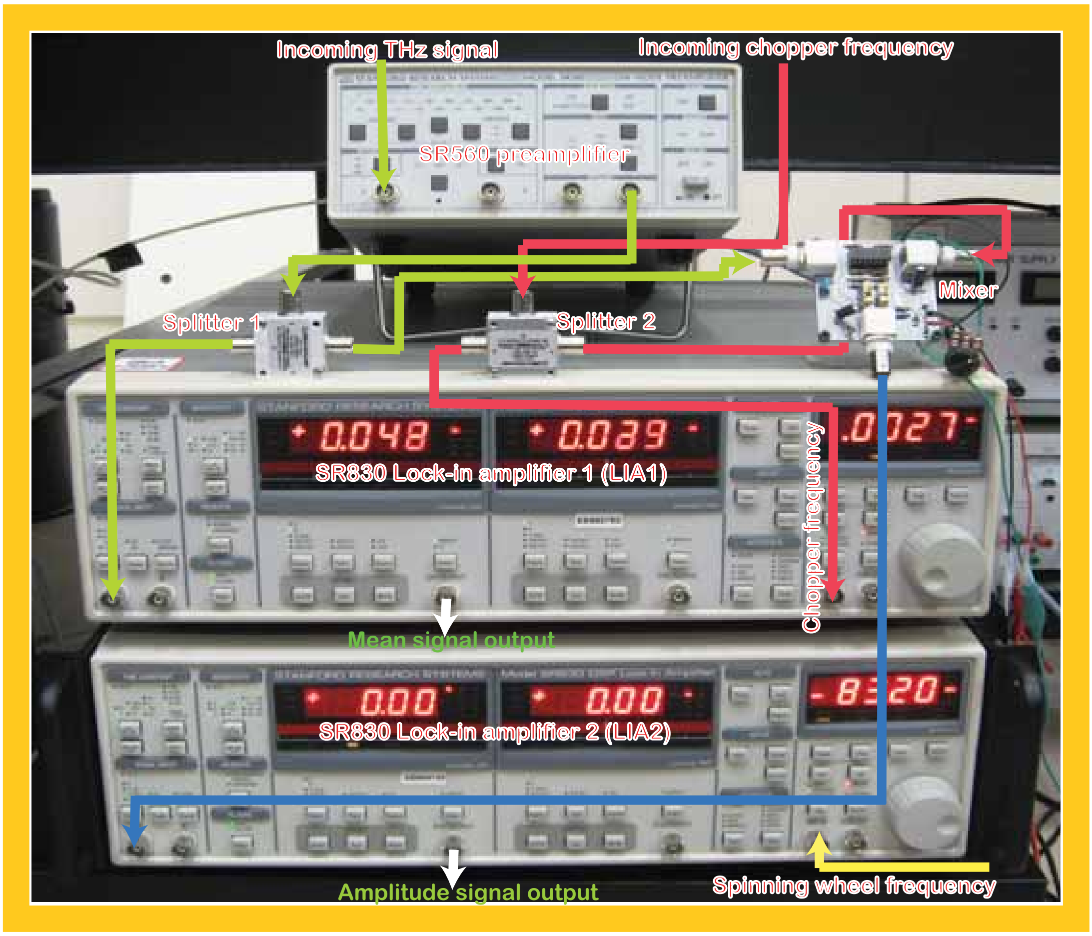

Figure C.8. Dual lock-in amplifier configuration. This photograph shows the lock-in amplifiers configuration for mean and amplitude signals extraction.

C.3.3 Spinning wheel

A novel custom-built spinning wheel device is depicted in Fig. C.9. The spinning wheel technique enables a rapid succesion of measurements between the reference and sample signals with a single mechanical delay scan. The main body of the spinning wheel is made from aluminium. The sample holder is made from a stainless-steel material to avoid contamination. A high speed brushless motor is attached to this device for spinning purposes. A photointerupter circuit and a interrupter disc are designed and attached at the back of device. This circuit and disc are used to convert the spinning speed in revolution per minute (rpm) into frequency (Hz).

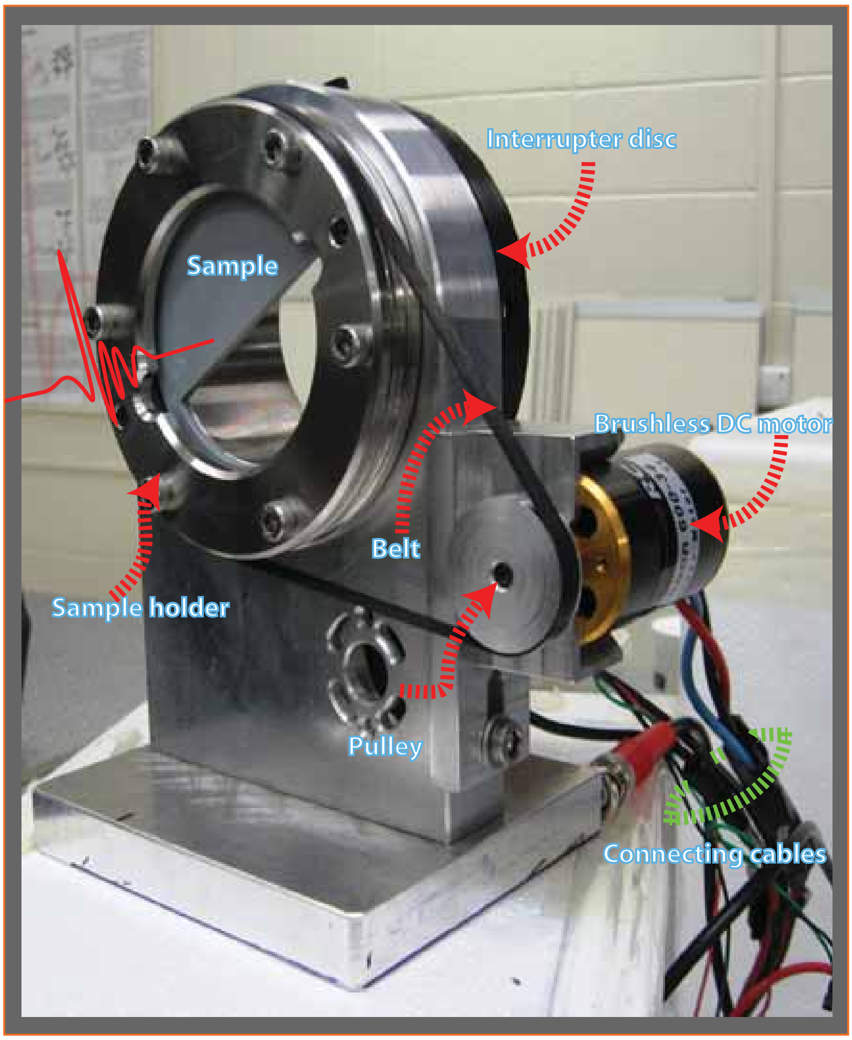

Figure C.9. The spinning wheel prototype. This figure depicts the spinning wheel device used for polymer material and liquid measurements discussed in Ch. 7 and 8.

C.4 Data acquisition for double-modulated THz-DTDS

Figure C.10 shows a screen shot of a LabVIEW program used to control a single motion controller and acquire terahertz signals (mean and amplitude signals) from two lock-in amplifiers simultaneously. The motion controller is connected to the computer terminal through the 10/100 Base-T Ethernet and the lock-in amplifiers are connected to the computer terminal through GPIB ribbon cable. The functionality of this program is similar to the one used in the conventional THz-TDS spectrometer, however,

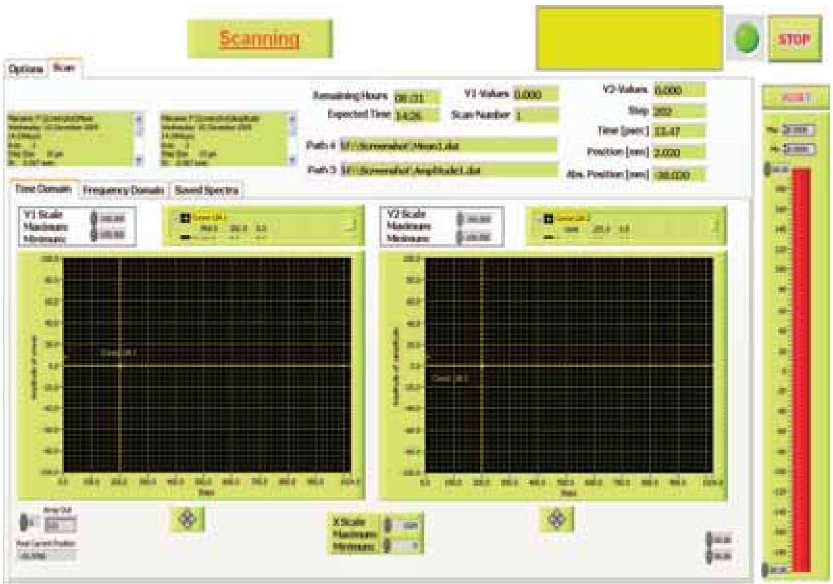

Figure C.10. Screen shot of LabVIEW program for double-modulated THz-DTDS spectrometer. This is a screen shot of the LabVIEW program developed to control the double-modulated THz-DTDS spectrometer. With this program, one may acquire mean and amplitude data simultaneously for analysis purposes. The graph indicators for acquiring the mean and amplitude signals are shown in the figure.

this program is modified to acquire mean and amplitude data simultaneously from the lock-in amplifiers. The data collected is then analysed using the Matlab software program described in Appendix D (see Sec. D.2).

Appendix D

Matlab Algorithms

THIS appendix presents some of the Matlab algorithms used in this thesis. These algorithms are available as m-files on the attached DVD-ROM. Examples of raw data files used in these algorithms are also attached.

D.1 Conventional THz-TDS analysis program

```
%%%%%%%%%%%%%%%%%%%%%%%%%%%%%%%%%%%%%%%%%%%%%%%%%%%%%%%%%%%%%%%%%%%%%%%%%%%%%%
% Program to analyse THz raw data. This program is written to extract THz %
%       material parameters through reference and sample signals.         %
%                                                                         %
% Jegathisvaran Balakrishnan                                              %
% The University of Adelaide                                              %
% December 2009                                                           %
%%%%%%%%%%%%%%%%%%%%%%%%%%%%%%%%%%%%%%%%%%%%%%%%%%%%%%%%%%%%%%%%%%%%%%%%%%%%%%

clear all;
c = 3E8;% Speed of light
d = 3E-3;% Thickness of the sample to be measured
Nscan = 6;% Number of scans
step=1024;% Number of steps for each scan

refmatrix_amp(step,Nscan) = 0;      % Intialize all the variables to zero %
refmatrix_time(step,Nscan) = 0;     %                                     %
sammatrix_amp(step,Nscan) = 0;      %                                     %
sammatrix_time(step,Nscan) = 0;     %                                     %
mean_smatrix_amp = 0;               %                                     %
mean_sammatrix_time = 0;            %                                     %
mean_rmatrix_amp = 0;               %                                     %
mean_refmatrix_time = 0;            %                                     %
mean_sample_absolute = 0;           %                                     %
mean_reference_absolute = 0;        %                                     %
mean_normal_phase = 0;              %                                     %
mean_match_phase = 0;               %                                     %
mean_transmission_absolute = 0;     %                                     %
mean_refractive_index = 0;          %                                     %
mean_absorption = 0;                %                                     %
standard_dev_refrac = 0;            %                                     %
standard_dev_absorp = 0;            %%%%%%%%%%%%%%%%%%%%%%%%%%%%%%%%%%%%%%%

for N = 1:Nscan
   %Import reference files for reading only
    disp(['Running reference ' int2str(N)]);
    fid = fopen(['reference_airtight' int2str(N) '.dat'],'r');
    reference_scan = textscan(fid,'%f %f ','headerlines',2);
    refmatrix_amp(:,N)= reference_scan{:,2};
    refmatrix_time(:,N) = reference_scan{:,1};
```

```
    fclose(fid);

   %Import sample files for reading only
    disp(['Running sample ' int2str(N)]);
    fid2 = fopen(['sample_80um' int2str(N) '.dat'],'r');
    reference_scan2 = textscan(fid2,'%f %f','headerlines',2);
    sammatrix_amp(:,N) = reference_scan2{:,2};
    sammatrix_time(:,N) = reference_scan2{:,1};
    fclose(fid2);

    zero_offsetA(:,N) = mean(refmatrix_amp(1:10,N));
    Rmatrix_amp(:,N) = refmatrix_amp(:,N)-zero_offsetA(:,N);
    zero_offsetB(:,N) = mean(sammatrix_amp(1:10,N));
    Smatrix_amp(:,N) = sammatrix_amp(:,N)-zero_offsetB(:,N);
    rmatrix_amp(:,N) = Rmatrix_amp(:,N);% Nth reference
    smatrix_amp(:,N) = Smatrix_amp(:,N);% Nth sample

    % Zero padding if it is necessary
    % for matupdateb=400:512
    %   rmatrix_amp(matupdateb,N) = 0;
    % end
    %
    % for matupdatea=400:512
    %   smatrix_amp(matupdatea,N) = 0;
    % end
    [m,n] = size(sammatrix_amp(:,1));
    timestep = mean(diff(sammatrix_time(1:m)));
    frequency = [0:m-1]'/timestep/m;

    % FFT of the reference and sample signals
    sample_fft(:,N) = fft(smatrix_amp(:,N));
    sample_absolute(:,N) = abs(sample_fft(:,N));
    reference_fft(:,N) = fft(rmatrix_amp(:,N));
    reference_absolute(:,N) = abs(reference_fft(:,N));

    % Transmission coefficient
    transmission(:,N) = sample_fft(:,N)./reference_fft(:,N);
    % The second element of the frequency gives the resolution.
    resolution = frequency(2);

    transmission_absolute(:,N) =abs(transmission(:,N));
```

```
% Unwrap the transmission angle followed by phase extrapolation
% for phase information extraction
transmission_phase(:,N) = -unwrap(angle(transmission(:,N)));
normal_phase(:,N) = transmission_phase(:,N);
lower_frequency = ceil(0.2/resolution);
upper_frequency = floor(0.45/resolution);
phase_difference(1,N) = transmission_phase(upper_frequency,N)
-transmission_phase(lower_frequency,N);

slope(1,N) = phase_difference(1,N)/(frequency(upper_frequency)
-frequency(lower_frequency));
yAxis(:,N) = slope(1,N)*frequency(1:lower_frequency);
j(1,N) = slope(1,N)*frequency(lower_frequency);
j2(1,N) = transmission_phase(lower_frequency,N);
diffj(1,N) = j(1,N)-j2(1,N);
a(:,N) = [yAxis(:,N)];
b(:,N) = [transmission_phase(lower_frequency+1:m,N)+diffj(1,N)];
match_phase(:,N) = [a(:,N); b(:,N)];% combining the a and b into matrix

%%%%%%%%%%%%%%%%%%%%%%%%%%%%%%%%%%%%%%%%%%%%%%%%%%%%%%%%%%%%%%%%%%%%%%%
% (1)Refractive index, extinction and absorption coefficient analysis %
%                     for dual-thickness geometry                    %
%%%%%%%%%%%%%%%%%%%%%%%%%%%%%%%%%%%%%%%%%%%%%%%%%%%%%%%%%%%%%%%%%%%%%%%

% omega = 2*pi*frequency*1*10^12;
% refractive_index(:,N) = c./(d.*omega).*match_phase(:,N)+1;
% extinction(:,N) = (c./(d*omega)').*log(transmission_absolute(:,N)');
% absorption_coefficient(:,N) = -(2/d)*log(transmission_absolute(:,N)');
% absorption(:,N) = absorption_coefficient(:,N)/100;

%%%%%%%%%%%%%%%%%%%%%%%%%%%%%%%%%%%%%%%%%%%%%%%%%%%%%%%%%%%%%%%%%%%%%%%
% (2)Refractive index, extinction and absorption coefficient analysis %
%            for air reference and sample (Used in Ch.4 and 5)        %
%%%%%%%%%%%%%%%%%%%%%%%%%%%%%%%%%%%%%%%%%%%%%%%%%%%%%%%%%%%%%%%%%%%%%%%

% omega = 2*pi*frequency*1*10^12;
% refractive_index(:,N) = 1+(c*match_phase(:,N)./(d*omega));
% absorption_coefficient(:,N) = -(2/d)*log((1+refractive_index(:,N))
% .*(1+refractive_index(:,N)).*transmission_absolute(:,N)./
% (4.*refractive_index(:,N)));
% absorption(:,N) = absorption_coefficient(:,N)/100;
```

```
%%%%%%%%%%%%%%%%%%%%%%%%%%%%%%%%%%%%%%%%%%%%%%%%%%%%%%%%%%%%%%%%%%%%%%%%
% (3)Refractive index, extinction and absorption coefficient analysis %
%         for  measurements with cell (transmission geometry (i))      %
%%%%%%%%%%%%%%%%%%%%%%%%%%%%%%%%%%%%%%%%%%%%%%%%%%%%%%%%%%%%%%%%%%%%%%%%

% omega = 2*pi*frequency*1*10^12;
% refractive_index(:,N) = 1+(c*match_phase(:,N)./(d*omega));
% absorption_coefficient(:,N) = -(2/d)*log((1.53+refractive_index(:,N))
% .*(1.53+refractive_index(:,N)).*transmission_absolute(:,N)./(6.4009.
% *refractive_index(:,N)));
% absorption(:,N) = absorption_coefficient(:,N)/100;


%%%%%%%%%%%%%%%%%%%%%%%%%%%%%%%%%%%%%%%%%%%%%%%%%%%%%%%%%%%%%%%%%%%%%%%%
% (4)Refractive index, extinction and absorption coefficient analysis %
%           for measurements with cell with air tight reference        %
%                      (transmission geometry (ii))                    %
%%%%%%%%%%%%%%%%%%%%%%%%%%%%%%%%%%%%%%%%%%%%%%%%%%%%%%%%%%%%%%%%%%%%%%%%

omega = 2*pi*frequency*1*10^12;
refractive_index(:,N) = c*match_phase(:,N)./(d*omega);
absorption_coefficient(:,N) = -(2/d)*log((1.53+refractive_index(:,N)).
*(1.53+refractive_index(:,N)).*transmission_absolute(:,N)./
(6.12.*refractive_index(:,N)));
absorption(:,N) = absorption_coefficient(:,N)/100;

%%%%%%%%%%%%%%%%%%%%%%%%%%%%%%%%%%%%%%%%%%%%%%%%%%%%%%%%%%%%%%%%%%%%%%%%
%     Plot the temporal shape of the reference and sample signals     %
%%%%%%%%%%%%%%%%%%%%%%%%%%%%%%%%%%%%%%%%%%%%%%%%%%%%%%%%%%%%%%%%%%%%%%%%

graph_one = figure(1);
subplot(2,1,1);
plot(sammatrix_time(:,N),smatrix_amp(:,N),'b','linewidth',1);
hold on
plot(refmatrix_time(:,N),rmatrix_amp(:,N),'b','linewidth',1);
grid on
xlabel('Time (ps)');
ylabel('Amplitude (a.u)');

%%%%%%%%%%%%%%%%%%%%%%%%%%%%%%%%%%%%%%%%%%%%%%%%%%%%%%%%%%%%%%%%%%%%%%%%
%   Plot the spectral amplitude of the reference and sample signals   %
%%%%%%%%%%%%%%%%%%%%%%%%%%%%%%%%%%%%%%%%%%%%%%%%%%%%%%%%%%%%%%%%%%%%%%%%
```

```
subplot(2,1,2);
semilogy(frequency(1:m/2),reference_absolute(1:m/2,N),'b','linewidth',1);
hold on
semilogy(frequency(1:m/2),sample_absolute(1:m/2,N),'b','linewidth',1);
grid on
xlabel('Frequency (THz)');
ylabel('Spectral amplitude (a.u)');

%%%%%%%%%%%%%%%%%%%%%%%%%%%%%%%%%%%%%%%%%%%%%%%%%%%%%%%%%%%%%%%%%%%%%%%%
%         Plot the original and extrapolated phase information       %
%%%%%%%%%%%%%%%%%%%%%%%%%%%%%%%%%%%%%%%%%%%%%%%%%%%%%%%%%%%%%%%%%%%%%%%%

graph_two = figure(2);
subplot(2,1,1);
plot(frequency(1:m/2),normal_phase(1:m/2,N),'b','linewidth',1);
hold on
plot(frequency(1:m/2),match_phase(1:m/2,N),'g','linewidth',1);
grid on
xlabel('Frequency (THz)');
ylabel('Phase (rad)');

%%%%%%%%%%%%%%%%%%%%%%%%%%%%%%%%%%%%%%%%%%%%%%%%%%%%%%%%%%%%%%%%%%%%%%%%
%                   Plot the transmission coefficient                %
%%%%%%%%%%%%%%%%%%%%%%%%%%%%%%%%%%%%%%%%%%%%%%%%%%%%%%%%%%%%%%%%%%%%%%%%

transmission_absolute(:,N) = transmission_absolute(:,N)*100;
subplot(2,1,2);
plot(frequency(1:m/2),transmission_absolute(1:m/2,N),'b','linewidth',1);
hold on
grid on
xlabel('Frequency (THz)');
ylabel('Transmission (%)');

graph_three = figure(3);
subplot(2,1,1);
plot(frequency(1:m/2),refractive_index(1:m/2,N),'b','linewidth',1);
grid on
xlabel('Frequency (THz)');
ylabel('refractive index (n)');

subplot(2,1,2);
```

```
    plot(frequency(1:m/2),absorption(1:m/2,N),'b','linewidth',1);
    grid on
    xlabel('Frequency (THz)');
    ylabel('Absorption coefficient (\alpha)');
end

mean_smatrix_amp = mean(smatrix_amp,2);
mean_sammatrix_time = mean(sammatrix_time,2);
mean_rmatrix_amp = mean(rmatrix_amp,2);
mean_refmatrix_time = mean(refmatrix_time,2);
mean_sample_absolute = mean(sample_absolute,2);
mean_reference_absolute = mean(reference_absolute,2);
mean_normal_phase = mean(normal_phase,2);
mean_match_phase = mean(match_phase,2);
mean_transmission_absolute = mean(transmission_absolute,2);
mean_refractive_index = mean(refractive_index,2);
mean_absorption = mean(absorption,2);
standard_dev_refrac = std(refractive_index,0,2);
standard_dev_absorp = std(absorption,0,2);
standard_dev_ref = std(rmatrix_amp,0,2);

% Plot the averaged terahertz reference and sample pulses in time domain.
graph_one = figure(1);
    subplot(2,1,1);plot(mean_refmatrix_time(1:m),mean_rmatrix_amp(1:m),'r',
    'linewidth',2);
    hold on
    plot(mean_refmatrix_time(1:m),mean_smatrix_amp(1:m),'g','linewidth',2);
    grid on
    legend('Reference','Sample',1);
    title('Temporal pulse shape for xxxx');
    xlabel('Time (ps)');
    ylabel('Amplitude (a.u)');

 % Plot the averaged spectral amplitude in frequency domain.
    subplot(2,1,2);
    semilogy(frequency(1:m/2),mean_reference_absolute(1:m/2),'r','linewidth',2);
    hold on
    semilogy(frequency(1:m/2),mean_sample_absolute(1:m/2),'g','linewidth',2);
    grid on
    legend('Reference','Sample',1);
    title('Spectral amplitude for xxxx');
    xlabel('Frequency (THz)');
```

```
    ylabel('Spectral amplitude (a.u)');

% Plot the averaged original and extrapolated phases in frequency domain.
graph_two = figure(2);
    subplot(2,1,1);
    plot(frequency(1:m/2),mean_normal_phase(1:m/2),'b','linewidth',2);
    hold on
    plot(frequency(1:m/2),mean_match_phase(1:m/2),'c','linewidth',2);
    grid on
    legend('Original','Extrapolated',1);
    title('Phase in frequency domain');
    xlabel('Frequency (THz)');
    ylabel('Phase (rad)');

% Plot the averaged transmission coefficient in frequency domain.
    subplot(2,1,2);
    plot(frequency(1:m/2),mean_transmission_absolute(1:m/2),'r','linewidth',1);
    grid on
    title('Transmission coefficient--absolute value (%)');
    xlabel('Frequency (THz)');
    ylabel('Transmission (%)');

% Plot the averaged, smoothed, and errorbar of the refractive index in
% frequency domain.
 graph_three = figure(3);
    subplot(2,1,1);
    plot(frequency(1:m/2),mean_refractive_index(1:m/2),'r','linewidth',2);
    hold on
        for s = 1:(m-2)
         average_REF (s) = mean((mean_refractive_index(s)
         +mean_refractive_index(s+1))/2);
    end
    errorbar(frequency(1:10:m/6),mean_refractive_index(1:10:m/6),
    standard_dev_refrac(1:10:m/6),'k','linewidth',1.5);
    hold on
    plot(frequency(1:m-2),average_REF(1:m-2),'g','linewidth',2);
    grid on
    title('Refractive index of xxxx  ')
    legend('Original','Error bar','Smoothed',1)
    xlabel('Frequency (THz)');
    ylabel('Refractive index (n)');
```

```
% Plot the averaged, smoothed, and errorbar of the absorption coefficient in
% frequency domain.
    subplot(2,1,2);
    plot(frequency(1:m/2),mean_absorption(1:m/2),'r','linewidth',1);
    hold on
    for s = 1:(m-2)
         average_abs (s) = mean((mean_absorption(s)+mean_absorption(s+1))/2);
    end
    errorbar(frequency(1:14:m/6),mean_absorption(1:14:m/6),
    standard_dev_absorp(1:14:m/6),'k','linewidth',2);
    hold on
    plot(frequency(1:m-2),average_abs(1:m-2),'g','linewidth',2);
    grid on
    title('Absorption coefficient of')
    legend('Original','Errorbar','Smoothed',1)
    xlabel('Frequency (THz)');
    ylabel('Absorption coefficient (\alpha)');

%%%%%%%%%%%%%%%%%%%%%%%%%%%%%%%%%%%%%%%%%%%%%%%%%%%%%%%%%%%%%%%%%%%%%%%%%%%%
%                            End of the program                            %
%%%%%%%%%%%%%%%%%%%%%%%%%%%%%%%%%%%%%%%%%%%%%%%%%%%%%%%%%%%%%%%%%%%%%%%%%%%%
```

D.2 Double-modulated THz-DTDS analysis program

```
%%%%%%%%%%%%%%%%%%%%%%%%%%%%%%%%%%%%%%%%%%%%%%%%%%%%%%%%%%%%%%%%%%%%%%%%%%%%
%  Program to analyse double-modulated THz-DTDS raw data. The program is  %
%  written to analyse mean and amplitude raw data obtained from the       %
%  double-modulated THz-DTDS measurements. The graphs for polymer         %
%  measurements and liquid measurements presented in Ch. 7 and Ch. 8 are  %
%  based on this program.                                                  %
%                                                                          %
%  Jegathisvaran Balakrishnan                                              %
%  The University of Adelaide                                              %
%  December 2009                                                           %
%%%%%%%%%%%%%%%%%%%%%%%%%%%%%%%%%%%%%%%%%%%%%%%%%%%%%%%%%%%%%%%%%%%%%%%%%%%%

clear all;
c = 3E8;                        % Speed of light.
d = 80E-6;                      % Thickness of the sample to be measured.
Nscan = 10;                     % Number of scans.
step=512;                       % Number of steps for each scan.

```

```
refmatrix_amp(step,Nscan) = 0;   % Intialize all the variables to zero.%
refmatrix_time(step,Nscan) = 0;  %                                     %
sammatrix_amp(step,Nscan) = 0;   %                                     %
sammatrix_time(step,Nscan) = 0;  %                                     %
mean_smatrix_amp = 0;            %                                     %
mean_sammatrix_time = 0;         %                                     %
mean_rmatrix_amp = 0;            %                                     %
mean_refmatrix_time = 0;         %                                     %
mean_sample_absolute = 0;        %                                     %
mean_reference_absolute = 0;     %                                     %
mean_normal_phase = 0;           %                                     %
mean_match_phase = 0;            %                                     %
mean_transmission_absolute = 0;  %                                     %
mean_refractive_index = 0;       %                                     %
mean_absorption = 0;             %                                     %
standard_dev_refrac = 0;         %                                     %
standard_dev_absorp = 0;         %                                     %
test = 0;                        %                                     %
test_real = 0;                   %                                     %
test_imag = 0;                   %                                     %
test_index = 0;                  %                                     %
test_alphax = 0;                 %                                     %
test_alpha = 0;                  %%%%%%%%%%%%%%%%%%%%%%%%%%%%%%%%%%%%%%%

% Importing measurement scans for analysis.
for N = 1:Nscan
   % Import mean files for reading only.
    disp(['Running mean ' int2str(N)]);
    fid = fopen(['Mean' int2str(N) '.dat'],'r');
    reference_scan = textscan(fid,'%f %f','headerlines',2);
    refmatrix_amp(:,N)= reference_scan{:,2};
    refmatrix_time(:,N) = reference_scan{:,1};
    fclose(fid);

   % Import amplitude files for reading only.
    disp(['Running amplitude ' int2str(N)]);
    fid2 = fopen(['Amplitude' int2str(N) '.dat'],'r');
    reference_scan2 = textscan(fid2,'%f %f','headerlines',2);
    sammatrix_amp(:,N) = reference_scan2{:,2};
    sammatrix_time(:,N) = reference_scan2{:,1};
    fclose(fid2);

```

```
% Introducing offset.
 zero_offsetA(:,N) = mean(refmatrix_amp(1:20,N));
 Rmatrix_amp(:,N) = refmatrix_amp(:,N)-zero_offsetA(:,N);

 zero_offsetB(:,N) = mean(sammatrix_amp(1:20,N));
 Smatrix_amp(:,N) = sammatrix_amp(:,N)-zero_offsetB(:,N);

% Calculating reference and sample signal through mean and amplitude raw
% data.
 rmatrix_amp(:,N) = Rmatrix_amp(:,N) + Smatrix_amp(:,N);
 smatrix_amp(:,N) = Rmatrix_amp(:,N) - Smatrix_amp(:,N);

 [m,n] = size(sammatrix_amp(:,1));
 timestep = mean(diff(sammatrix_time(1:m)));
 frequency = [0:m-1]'/timestep/m;
 sample_fft(:,N) = fft(smatrix_amp(:,N));
 sample_absolute(:,N) = abs(sample_fft(:,N));
 reference_fft(:,N) = fft(rmatrix_amp(:,N));
 reference_absolute(:,N) = abs(reference_fft(:,N));

% Transmission coefficient
 transmission(:,N) = sample_fft(:,N)./reference_fft(:,N);

% The second element of the freqeuncy gives the resolution.
 resolution = frequency(2);

 transmission_absolute(:,N) =abs(transmission(:,N));

% Unwrap the transmission angle for phase.
 transmission_phase(:,N) = -unwrap(angle(transmission(:,N)));
 normal_phase(:,N) = transmission_phase(:,N);

% Detemine the lower frequency element.
 lower_frequency = ceil(0.2/resolution);

% Determine the upper frequency element.
 upper_frequency = floor(0.5/resolution);

% Phase extrapolation.
 phase_difference(1,N) = transmission_phase(upper_frequency,N)
 -transmission_phase(lower_frequency,N);
 slope(1,N) = phase_difference(1,N)/(frequency(upper_frequency)
```

```
    -frequency(lower_frequency));
    yAxis(:,N) = slope(1,N)*frequency(1:lower_frequency);
    j(1,N) = slope(1,N)*frequency(lower_frequency);
    j2(1,N) = transmission_phase(lower_frequency,N);
    diffj(1,N) = j(1,N)-j2(1,N);
    a(:,N) = [yAxis(:,N)];
    b(:,N) = [transmission_phase(lower_frequency+1:m,N)+diffj(1,N)];
    match_phase(:,N) = [a(:,N); b(:,N)];

%%%%%%%%%%%%%%%%%%%%%%%%%%%%%%%%%%%%%%%%%%%%%%%%%%%%%%%%%%%%%%%%%%%%%%%%
%   Refractive index, extinction and absorption coefficient analysis  %
%     for reference and sample (dual-thickness liquid measurement).   %
%                                                                      %
%%%%%%%%%%%%%%%%%%%%%%%%%%%%%%%%%%%%%%%%%%%%%%%%%%%%%%%%%%%%%%%%%%%%%%%%

omega = 2*pi*frequency*1*10^12;
refractive_index(:,N) = c./(d.*omega).*match_phase(:,N)+1;
extinction(:,N) = (c./(d*omega)').*log(transmission_absolute(:,N)');
absorption_coefficient(:,N) = -(2/d)*log(transmission_absolute(:,N)');
absorption(:,N) = absorption_coefficient(:,N)/100;


%%%%%%%%%%%%%%%%%%%%%%%%%%%%%%%%%%%%%%%%%%%%%%%%%%%%%%%%%%%%%%%%%%%%%%%%
%   Refractive index, extinction and absorption coefficient analysis  %
%     for reference and sample (polymer measurement).                 %
%                                                                      %
%%%%%%%%%%%%%%%%%%%%%%%%%%%%%%%%%%%%%%%%%%%%%%%%%%%%%%%%%%%%%%%%%%%%%%%%

% omega = 2*pi*frequency*1*10^12;
% refractive_index(:,N) = 1+(c*match_phase(:,N)./(d*omega));
% absorption_coefficient(:,N) = -(2/d)*log((1+refractive_index(:,N)).*
% (1+refractive_index(:,N)).*transmission_absolute(:,N)./
% (4.*refractive_index(:,N)));
% absorption(:,N) = absorption_coefficient(:,N)/100;

%%%%%%%%%%%%%%%%%%%%%%%%%%%%%%%%%%%%%%%%%%%%%%%%%%%%%%%%%%%%%%%%%%%%%%%%
% Double Debye relaxation model for liquid measurement. The fitting   %
% parameters are ontained from J. T. Kindt et. al (1996).             %
%%%%%%%%%%%%%%%%%%%%%%%%%%%%%%%%%%%%%%%%%%%%%%%%%%%%%%%%%%%%%%%%%%%%%%%%

%Double Debye model for water
test =  3.48 + (78.36-4.93)./(1-8.24*10^(-12)*omega*i) + (4.93-3.48)./
```

```
 (1-0.182*10^(-12)*omega*i);

 %%%%%%%%%%%%%%%%%%%%%%%%%%%%%%%%%%%%%%%%%%%%%%%%%%%%%%%%%%%%%%%%%%%%%%%%
 % Triple Debye relaxation model for liquid measurement. The fitting   %
 % parameters are ontained from J. T. Kindt et. al (1996).             %
 %%%%%%%%%%%%%%%%%%%%%%%%%%%%%%%%%%%%%%%%%%%%%%%%%%%%%%%%%%%%%%%%%%%%%%%%

 %Double Debye model for ethanol
 % test  = 1.93 + (24.35-4.15)./(1+161*10^(-12)*omega*i) + (4.15-2.72)./
 %(1+3.3*10^(-12)*omega*i)+(2.72-1.93)./(1+0.22*10^(-12)*omega*i);

 %Double Debye model for methanol
 %test  = 2.10 + (32.63-5.35)./(1+48*10^(-12)*omega*i) + (5.35-3.37)./
 %(1+1.25*10^(-12)*omega*i)+(3.37-2.10)./(1+0.16*10^(-12)*omega*i);

 test_real =  real(test);
 test_imag =  imag(test);
 test_index = sqrt(((sqrt((test_real.*test_real)+(test_imag.*test_imag)))
 + test_real)*0.5);

 test_alphax =2.*omega./c;
 test_alpha = (test_alphax.*sqrt(((sqrt((test_real.*test_real)
 + (test_imag.*test_imag))) - test_real)*0.5))/100;

% Plot the terahertz reference and sample pulses in time domain.
 graph_one = figure(1);
 subplot(2,1,1);
 plot(sammatrix_time(:,N),smatrix_amp(:,N),'b','linewidth',1);
 hold on
 plot(refmatrix_time(:,N),rmatrix_amp(:,N),'b','linewidth',1);
 grid on

% Plot the spectral amplitude in frequency domain.
 subplot(2,1,2);
 semilogy(frequency(1:m/2),reference_absolute(1:m/2,N),'b','linewidth',1);
 hold on
 semilogy(frequency(1:m/2),sample_absolute(1:m/2,N),'b','linewidth',1);
 grid on

% Plot the original and extrapolated phases in frequency domain.
 graph_two = figure(2);
 subplot(2,1,1);
```

```
    plot(frequency(1:m/2),normal_phase(1:m/2,N),'b','linewidth',1);
    hold on
    plot(frequency(1:m/2),match_phase(1:m/2,N),'g','linewidth',1);
    grid on

   % Plot the transmission coefficient in frequency domain.
    transmission_absolute(:,N) = transmission_absolute(:,N)*100;

    subplot(2,1,2);
    plot(frequency(1:m/2),transmission_absolute(1:m/2,N),'b','linewidth',1);
    grid on

   % Comparison of refractive index obtained from the measurement with the
   % refractive index obtained from the Debye relaxation model.

    graph_three = figure(3);
    subplot(2,1,1);
    plot(frequency(1:m/2),refractive_index(1:m/2,N),'b','linewidth',1);
    hold on
    plot(frequency(1:m-2),test_index(1:m-2),'b','linewidth',2);
    grid on

   % Comparison of absorption coefficient obtained from the measurement with
   % the absorption coefficient obtained from the Debye relaxation model.
    subplot(2,1,2);
    plot(frequency(1:m/2),absorption(1:m/2,N),'b','linewidth',1);
    hold on
    plot(frequency(1:m-2),test_alpha(1:m-2),'b','linewidth',2);
    grid on

end

mean_smatrix_amp = mean(smatrix_amp,2);
mean_sammatrix_time = mean(sammatrix_time,2);
mean_rmatrix_amp = mean(rmatrix_amp,2);
mean_refmatrix_time = mean(refmatrix_time,2);
mean_sample_absolute = mean(sample_absolute,2);
mean_reference_absolute = mean(reference_absolute,2);
mean_normal_phase = mean(normal_phase,2);
mean_match_phase = mean(match_phase,2);
mean_transmission_absolute = mean(transmission_absolute,2);
mean_refractive_index = mean(refractive_index,2);
```

```
mean_absorption = mean(absorption,2);

% Calculating standard deviation for the refractive index
standard_dev_refrac = std(refractive_index,0,2);

% Calculating standard deviation for the absorption coeff
standard_dev_absorp = std(absorption,0,2);


% Plot the averaged terahertz reference and sample pulses in time domain.
graph_one = figure(1);
    subplot(2,1,1);plot(mean_refmatrix_time(1:m/2),mean_rmatrix_amp(1:m/2)
    ,'r','linewidth',2);
    hold on
    plot(mean_refmatrix_time(1:m/2),mean_smatrix_amp(1:m/2),'g','linewidth'
    ,2);
    grid on
    legend('Reference','Sample',1);
    title('Temporal pulse shape of xxx');
    xlabel('Time (ps)');
    ylabel('Amplitude (a.u)');

% Plot the averaged spectral amplitude in frequency domain.
    subplot(2,1,2);
    semilogy(frequency(1:m/2),mean_reference_absolute(1:m/2),'r','linewidth',2);
    hold on
    semilogy(frequency(1:m/2),mean_sample_absolute(1:m/2),'g','linewidth',2);
    grid on
    legend('Reference','Sample',1);
    title('Spectral amplitude of xxx');
    xlabel('Frequency (THz)');
    ylabel('Spectral amplitude (a.u)');

% Plot the averaged original and extrapolated phases in frequency domain.
graph_two = figure(2);
    subplot(2,1,1);
    plot(frequency(1:m/2),mean_normal_phase(1:m/2),'b','linewidth',2);
    hold on
    plot(frequency(1:m/2),mean_match_phase(1:m/2),'c','linewidth',2);
    grid on
    legend('Original','Extrapolated',1);
    title('Phase of xxx');
```

```
   xlabel('Frequency (THz)');
   ylabel('Phase (rad)');

% Plot the averaged  transmission coefficient in frequency domain.
   subplot(2,1,2);
   plot(frequency(1:m/2),mean_transmission_absolute(1:m/2),'r','linewidth',1);
   grid on
   title('Transmission coefficient of xxx');
   xlabel('Frequency (THz)');
   ylabel('Transmission (%)');

% Plot the averaged, smoothed, and errorbar of the refractive index in
% frequency domain.
graph_three = figure(3);
   subplot(2,1,1);
   plot(frequency(1:m/2),mean_refractive_index(1:m/2),'r','linewidth',2);
   hold on
   for s = 1:(m-2)
        average_REF (s) = mean((mean_refractive_index(s)+mean_refractive_index
        (s+1))/2);
   end
   errorbar(frequency(1:10:m/6),mean_refractive_index(1:10:m/6),
   standard_dev_refrac(1:10:m/6),'k','linewidth',1.5);
   hold on
   plot(frequency(1:m-2),average_REF(1:m-2),'g','linewidth',2);
   grid on
   title('Refractive index of xxx ')
   legend('Original','Smoothed',1)
   xlabel('Frequency (THz)');
   ylabel('Refractive index (n)');

% Plot the averaged, smoothed, and errorbar of the absorption coefficient in
% frequency domain.
   subplot(2,1,2);
   plot(frequency(1:m/2),mean_absorption(1:m/2),'r','linewidth',1);
   hold on
   for s = 1:(m-2)
        average_abs (s) = mean((mean_absorption(s)+mean_absorption(s+1))/2);
   end
   errorbar(frequency(1:14:m/6),mean_absorption(1:14:m/6),
   standard_dev_absorp(1:14:m/6),'k','linewidth',2);
   hold on
```

```
    plot(frequency(1:m-2),average_abs(1:m-2),'g','linewidth',2);
    grid on
    title('Absorption coefficient of xxx')
    legend('Original','Smoothed',1)
    xlabel('Frequency (THz)');
    ylabel('Absorption coefficient (\alpha)');

%%%%%%%%%%%%%%%%%%%%%%%%%%%%%%%%%%%%%%%%%%%%%%%%%%%%%%%%%%%%%%%%%%%%%%%%%%%%%%%%
%                              End of the program                              %
%%%%%%%%%%%%%%%%%%%%%%%%%%%%%%%%%%%%%%%%%%%%%%%%%%%%%%%%%%%%%%%%%%%%%%%%%%%%%%%%
```

D.3 Modelling conventional THz-TDS signal extraction

```
%%%%%%%%%%%%%%%%%%%%%%%%%%%%%%%%%%%%%%%%%%%%%%%%%%%%%%%%%%%%%%%%%%%%%%%%%%%%%%%%
%      Simulation program to model terahertz signal extraction from a          %
%                    conventional THz-TDS spectrometer.                        %
%                                                                              %
% Jegathisvaran Balakrishnan                                                   %
% The University of Adelaide                                                   %
% December 2009                                                                %
%%%%%%%%%%%%%%%%%%%%%%%%%%%%%%%%%%%%%%%%%%%%%%%%%%%%%%%%%%%%%%%%%%%%%%%%%%%%%%%%

clear all;
% Load original signal for simulation
fid1 = fopen('Simulation\xxxx','r');
reference_scan1 = textscan(fid1,'%f %f','headerlines',2);
reference_amplitude1 = reference_scan1{:,2};
reference_time1 = reference_scan1{:,1};
fclose(fid1);

[m,n] = size(reference_amplitude1(:,1));
timestep = mean(diff(reference_time1(1:m)))./10;

fs = 10000; % Sampling frequency
fc = 0.35; % cutoff frequency
∆ = timestep;
num_sam = m;
time = (0:num_sam-1)*∆; %time axis
frequency = [0:num_sam-1]'/∆/num_sam;
chopperfreq = 2.0;% chopper frequency in Hz
fchopper = sin(2*pi*chopperfreq*time);

```

```
nth = 6;% filter order
%harmonics generation using for loop is require to create square wave out
%of sine wave
for k = 2:3
    fchopper = fchopper + sin(((2*k)-1).*2*pi*chopperfreq*time)/((2*k)-1);
end
fchopper = (fchopper*4)/pi;

% nth order low pass Butterworth filter
[B A] = butter(nth,fc/(fs/80));
h = freqs(B,A,frequency);
mag = 20*log10(abs(h));
figure(1);
semilogx(frequency,mag)
xlabel('Frequency in Hz');
ylabel('Magnitude (dB)');

detector=[];
lock_in_t=[];
lock_in_nt=[];
lock_in_fft_nt=[];
butter_gaussian=[];
butter_gaussian_fft=[];
inverse_origin_fft=[];
inverse_gaussian_fft=[];

% modulated raw output without noise
for s = 1:length(reference_amplitude1)
    for s1 = 1:length(fchopper)
        detector(s,s1) = (fchopper(s1).*reference_amplitude1(s));
    end
end

% demodulated output without noise
for s = 1:length(reference_amplitude1)
    for s1 = 1:length(fchopper)
        lock_in_t(s,s1) = (detector(s,s1)*fchopper(s1));
    end
end

% Add white noise to the modulated signal
for s = 1:length(reference_amplitude1)
```

```
    testDt = [];
    testDt = awgn(detector(s,:),10,'measured');
    for s1 = 1:length(fchopper)
        detector_nt(s,s1) = testDt(s1);
    end
end

% Add white noise to the demodulated signal
for s = 1:length(reference_amplitude1)
    testD = [];
    testD = awgn(lock_in_t(s,:),10,'measured');
    for s1 = 1:length(fchopper)
        lock_in_nt(s,s1) = testD(s1);
    end
end

% FFT the noise added modulated signal
for s = 1:length(reference_amplitude1)
    signoisedt = [];
    signoisedt = fft(detector_nt(s,:));
    for s1 = 1:length(fchopper)
        detector_fft_nt(s,s1) = signoisedt(s1);
    end
end

% FFT the noise added demodulated signal
for s = 1:length(reference_amplitude1)
    signoise = [];
    signoise = fft(lock_in_nt(s,:));
    for s1 = 1:length(fchopper)
        lock_in_fft_nt(s,s1) = signoise(s1);
    end
end

% Apply butterworth nth order filter to introduce 1/f noise
for s = 1:length(reference_amplitude1)
    testE = [];
    testE = filter(B,A,lock_in_nt(s,:));
    for s1 = 1:length(fchopper)
        butter_gaussian(s,s1) = testE(s1);
    end
end
```

```
% FFT the butterworth nth order filter
for s = 1:length(reference_amplitude1)
    testF = [];
    testF = fft(butter_gaussian(s,:));
    for s1 = 1:length(fchopper)
        butter_gaussian_fft(s,s1) = testF(s1);
    end
end



% Inverse FFT of the filter for recovering the original signal after filtering
for s = 1:length(reference_amplitude1)
    testG = [];
    testG = ifft(butter_gaussian_fft(s,:));
    for s1 = 1:length(fchopper)
        inverse_gaussian_fft(s,s1) = testG(s1);
    end
end

% Recovering the averaged original input signal after filtering
y=[];
for s = 1:length(reference_amplitude1)
y(s) = mean(inverse_gaussian_fft(s,:));
end

% Plot the modulated, demodulated, butterworth low-pass filtered signals in
% time domain
pause
graph2 = figure(2);
subplot(2,1,1);plot(time,detector(150,:),'r');
hold on
plot(time,lock_in_nt(150,:),'b');
hold on
plot(time,butter_gaussian(150,:),'g');
legend('Modulated signal','Demodulated signal','Butterworth LPF');
xlabel('Time in sec');
ylabel('Amplitude (a.u)');
title('Before and after butterworth low-pass filter at 150th step of the
delay stage');
```

```
% Plot the modulated, demodulated, butterworth low-pass filtered signals in
% frequency domain

subplot(2,1,2);plot(frequency,abs(detector_fft_nt(150,:)),'r');
hold on
plot(frequency,abs(lock_in_fft_nt(150,:)),'b');
hold on
plot(frequency,abs(butter_gaussian_fft(150,:)),'g');
legend('Modulated signal','Demodulated signal','Butterworth LPF');
xlabel('Frequency in Hz');
ylabel('Amplitude (a.u)');
title('Before and after butterworth low-pass filter at 150th step of the
delay stage');

% Plot the original signal and compare it the signal recovered after
% filtering process
pause
graph3 = figure(3);
plot(time,reference_amplitude1,'b')
hold on
plot(time,y,'r');
xlabel('Time in sec');
ylabel('Amplitude (a.u)');
title('Original signal','Recovered terahertz signal');
```

D.4 Modelling double-modulated THz-DTDS signal extraction

```
%%%%%%%%%%%%%%%%%%%%%%%%%%%%%%%%%%%%%%%%%%%%%%%%%%%%%%%%%%%%%%%%%%%%%%%%%%%
%           Simulation program to model terahertz signal extraction      %
%             from a double-modulated terahertz double-modulated         %
%                  differential time-domain spectroscopy.                 %
%                                                                        %
% Jegathisvaran Balakrishnan                                             %
% The University Adelaide                                                %
% December 2009                                                          %
%%%%%%%%%%%%%%%%%%%%%%%%%%%%%%%%%%%%%%%%%%%%%%%%%%%%%%%%%%%%%%%%%%%%%%%%%%%

clear all;
% Load mean signal for simulation
fid1 = fopen('Simulation\Mean.dat','r');
```

```
reference_scan1 = textscan(fid1,'%f %f','headerlines',2);
reference_amplitude1 = reference_scan1{:,2};
reference_time1 = reference_scan1{:,1};
fclose(fid1);

% Load amplitude signal for simulation
fid2 = fopen('Simulation\Amplitude.dat','r');
reference_scan2 = textscan(fid2,'%f %f','headerlines',2);
reference_amplitude2 = reference_scan2{:,2};
reference_time2 = reference_scan2{:,1};
fclose(fid2);

[m,n] = size(reference_amplitude1(:,1));
timestep = mean(diff(reference_time1(1:m)))./10;

fs = 100000; % sampling frequency
fc = 0.8; % cutoff frequency
Δ = timestep;
num_sam = m;
time = (0:num_sam-1)*Δ; %time axis
frequency = [0:num_sam-1]'/Δ/num_sam;
chopperfreq = 3.0;% chopper frequency in Hz
fchopper = sin(2*pi*chopperfreq*time);
wheelfreq = 0.5;% wheel frequency in Hz
fwheel = sin(2*pi*rotatorfreq*time);
nth = 1;% filter order

% harmonics generation using for loop is require to create square wave out
% of sine wave
 for k = 2:2
    fchopper = fchopper + sin((2*k-1).*2*pi*chopperfreq*time)/((2*k)-1);
    fwheel = fwheel + sin((2*k-1).*2*pi*wheelfreq*time)/((2*k)-1);
 end
fchopper = (fchopper*4)/pi+1;
fwheel = (fwheel*4)/pi+1;

% Equation 10.9 in Ch. 10. Simulated double-modulated terahertz signal
% at the detector
Amp=max(fwheel); % Reference thickness
xTh=0.2;         % Sample thickness
fwheel2=[]; fcpct=1;
for fchct=1:length(fwheel)
```

```
    fwheel2(fcpct)=(((Amp-xTh)/Amp)*fwheel(fchct))+xTh;
    fcpct=fcpct+1;
end
fmod = fchopper.*frotator2;

%%%%%%%%%%%%%%%%%%%%%%%%%%%%%%%%%%%%%%%%%%%%%%%%%%%%%%%%%%%%%%%%%%%%%%%%%%%

% nth order low pass Butterworth filter
[B A] = butter(nth,fc/(fs/80));
h = freqs(B,A,frequency);
mag = 20*log10(abs(h));
figure(1);
semilogx(frequency,mag)
xlabel('Frequency in Hz');
ylabel('Magnitude (dB)');


%%%%%%%%%%%%%%%%%%%%%%%%%%%%%%%%%%%%%%%%%%%%%%%%%%%%%%%%%%%%%%%%%%%%%%%%%%%
%            Recovering mean signal without introducing any noise          %
%%%%%%%%%%%%%%%%%%%%%%%%%%%%%%%%%%%%%%%%%%%%%%%%%%%%%%%%%%%%%%%%%%%%%%%%%%%
detector=[];
detector_fft_t=[];
lock_in_t=[];
lock_in_fft_t=[];
lock_in_fft_nt=[];
butter_origin =[];
butter_origin_fft=[];
butter_gaussian=[];
butter_gaussian_fft=[];
inverse_origin_fft=[];
inverse_gaussian_fft=[];
lock_in_nt=[];

% Double-modulated raw output without noise
for s = 1:length(reference_amplitude1)
    for s1 = 1:length(fchopper)
        detector(s,s1) = fmod(s1).*reference_amplitude1(s);
    end
end

% FFT of the double-modulated raw output without noise
for s = 1:length(reference_amplitude1)
```

```
    sigdt = [];
    sigdt = fft(detector(s,:));
    for s1 = 1:length(fchopper)
        detector_fft_t(s,s1) = sigdt(s1);
    end
end

% Demodulated signal without any filtering and noise (mixer output, LIA1
% PSD output)
for s = 1:length(reference_amplitude1)
    for s1 = 1:length(fchopper)
        lock_in_t(s,s1) = detector(s,s1)*fchopper(s1);
    end
end

% FFT Demodulated signal without any filtering and noise (mixer output,
% LIA1 PSD output)
for s = 1:length(reference_amplitude1)
    sigX = [];
    sigX = fft(lock_in_t(s,:));
    for s1 = 1:length(fchopper)
        lock_in_fft_t(s,s1) = sigX(s1);
    end
end

% Apply butterworth nth order filter to extract mean signal
for s = 1:length(reference_amplitude1)
    testA = [];
    testA = filter(B,A,lock_in_t(s,:));
    for s1 = 1:length(fchopper)
        butter_origin(s,s1) = testA(s1);
    end
end

% FFT the butterworth nth order filter
for s = 1:length(reference_amplitude1)
    testB = [];
    testB = fft(butter_origin(s,:));
    for s1 = 1:length(fchopper)
        butter_origin_fft(s,s1) = testB(s1);
    end
end
```

```
% Inverse FFT of the filter for recovering the original mean signal after
% filtering
for s = 1:length(reference_amplitude1)
    testC = [];
    testC = ifft(butter_origin_fft(s,:));
    for s1 = 1:length(fchopper)
        inverse_origin_fft(s,s1) = testC(s1);
    end
end

%%%%%%%%%%%%%%%%%%%%%%%%%%%%%%%%%%%%%%%%%%%%%%%%%%%%%%%%%%%%%%%%%%%%%%%%%%%%%%
%         Recovering amplitude signal without introducing any noise        %
%%%%%%%%%%%%%%%%%%%%%%%%%%%%%%%%%%%%%%%%%%%%%%%%%%%%%%%%%%%%%%%%%%%%%%%%%%%%%%

% Demodulate the mixer output with fwheel(spinning whee)
for s = 1:length(reference_amplitude1)
    for s1 = 1:length(fchopper)
        lock_2in_t(s,s1) = (lock_in_t(s,s1)*fwheel(s1));
    end
end

% FFT of the demodulated output signal
for s = 1:length(reference_amplitude1)
    sig = [];
    sig = fft(lock_2in_t(s,:));
    for s1 = 1:length(fchopper)
        lock_2in_fft_t(s,s1) = sig(s1);
    end
end

% Apply butterworth nth order filter to extract amplitude signal
for s = 1:length(reference_amplitude1)
    testAx = [];
    testAx = filter(B,A,lock_2in_t(s,:));
    for s1 = 1:length(fchopper)
        butter_2origin(s,s1) = testAx(s1);
    end
end

% FFT the butterworth nth order filter
for s = 1:length(reference_amplitude1)
```

```
    testBx = [];
    testBx = fft(butter_2origin(s,:));
    for s1 = 1:length(fchopper)
        butter_2origin_fft(s,s1) = testBx(s1);
    end
end

% Inverse FFT of the filter for recovering the original amplitude signal after
% filtering
for s = 1:length(reference_amplitude1)
    testCx = [];
    testCx = ifft(butter_2origin_fft(s,:));
    for s1 = 1:length(fchopper)
        inverse_2origin_fft(s,s1) = testCx(s1);
    end
end

%%%%%%%%%%%%%%%%%%%%%%%%%%%%%%%%%%%%%%%%%%%%%%%%%%%%%%%%%%%%%%%%%%%%%%%%%%%
%                Recovering mean signal with Gaussian noise               %
%%%%%%%%%%%%%%%%%%%%%%%%%%%%%%%%%%%%%%%%%%%%%%%%%%%%%%%%%%%%%%%%%%%%%%%%%%%

% Adding gaussian noise on the double-modulated signal
for s = 1:length(reference_amplitude1)
    testDt = [];
    testDt = awgn(detector(s,:),10,'measured');
    for s1 = 1:length(fchopper)
        detector_nt(s,s1) = testDt(s1);
    end
end

% FFT the double-modulated signal with noise Gaussian noise
for s = 1:length(reference_amplitude1)
    signoisedt = [];
    signoisedt = fft(detector_nt(s,:));
    for s1 = 1:length(fchopper)
        detector_fft_nt(s,s1) = signoisedt(s1);
    end
end

% Adding gaussian noise to the demodulated signal
for s = 1:length(reference_amplitude1)
    testD = [];
```

```
    testD = awgn(lock_in_t(s,:),10,'measured');
    for s1 = 1:length(fchopper)
        lock_in_nt(s,s1) = testD(s1);
    end
end

% FFT the demodulated signal
for s = 1:length(reference_amplitude1)
    signoise = [];
    signoise = fft(lock_in_nt(s,:));
    for s1 = 1:length(fchopper)
        lock_in_fft_nt(s,s1) = signoise(s1);
    end
end

% Apply butterworth nth order filter to extract mean signal
for s = 1:length(reference_amplitude1)
    testE = [];
    testE = filter(B,A,lock_in_nt(s,:));
    for s1 = 1:length(fchopper)
        butter_gaussian(s,s1) = testE(s1);
    end
end

% FFT the butterworth filtered mean signal
for s = 1:length(reference_amplitude1)
    testF = [];
    testF = fft(butter_gaussian(s,:));
    for s1 = 1:length(fchopper)
        butter_gaussian_fft(s,s1) = testF(s1);
    end
end

% Inverse FFT to recover the original mean signal
for s = 1:length(reference_amplitude1)
    testG = [];
    testG = ifft(butter_gaussian_fft(s,:));
    for s1 = 1:length(fchopper)
        inverse_gaussian_fft(s,s1) = testG(s1);
    end
end
```

```
%%%%%%%%%%%%%%%%%%%%%%%%%%%%%%%%%%%%%%%%%%%%%%%%%%%%%%%%%%%%%%%%%%%%%%%%%%%%%%%%%
%               Recovering amplitude signal with Gaussian noise          %
%%%%%%%%%%%%%%%%%%%%%%%%%%%%%%%%%%%%%%%%%%%%%%%%%%%%%%%%%%%%%%%%%%%%%%%%%%%%%%%%%

% Adding gaussian noise to the demodulated signal of lock-in amplifier two
% (PSD output of lock-in amplifier two)
for s = 1:length(reference_amplitude1)
    testDx = [];
    testDx = awgn(lock_2in_t(s,:),10,'measured');
    for s1 = 1:length(fchopper)
        lock_2in_nt(s,s1) = testDx(s1);
    end
end

% FFT the PSD output of lock-in amplifier two
for s = 1:length(reference_amplitude1)
    signoiseX = [];
    signoiseX = fft(lock_2in_nt(s,:));
    for s1 = 1:length(fchopper)
        lock_2in_fft_nt(s,s1) = signoiseX(s1);
    end
end

% Introducing butterworth filtering to the PSD out signal
for s = 1:length(reference_amplitude1)
    testEx = [];
    testEx = filter(B,A,lock_2in_nt(s,:));
    for s1 = 1:length(fchopper)
        butter_2gaussian(s,s1) = testEx(s1);
    end
end

% FFT of the filtered signal
for s = 1:length(reference_amplitude1)
    testFx = [];
    testFx = fft(butter_2gaussian(s,:));
    for s1 = 1:length(fchopper)
        butter_2gaussian_fft(s,s1) = testFx(s1);
    end
end

% Inverse FFT of the filtered signal to recover the original input
```

```matlab
% amplitude signal
for s = 1:length(reference_amplitude1)
    testGx = [];
    testGx = ifft(butter_2gaussian_fft(s,:));
    for s1 = 1:length(fchopper)
        inverse_2gaussian_fft(s,s1) = testGx(s1);
    end
end

% Averaging the inverse FFT of the filtered mean signal
y=[];
for s = 1:length(reference_amplitude1)
y(s) = mean(inverse_gaussian_fft(s,:));
end

% Averaging the inverse FFT of the filtered amplitude signal
h=[];
for s = 1:length(reference_amplitude1)
h(s) = mean(inverse_2gaussian_fft(s,:));
end

%%%%%%%%%%%%%%%%%%%%%%%%%%%%%%%%%%%%%%%%%%%%%%%%%%%%%%%%%%%%%%%%%%%%%%%%%%%
%                Plot signals in time and frequency domains               %
%%%%%%%%%%%%%%%%%%%%%%%%%%%%%%%%%%%%%%%%%%%%%%%%%%%%%%%%%%%%%%%%%%%%%%%%%%%
pause
graph2 = figure(2);

% Plot the fchopper signal and fwheel2 signal in time domain
subplot(2,1,1);
plot(time,fchopper,'g');
hold on
plot(time,fwheel2,'b');
legend('Chopper frequency','Spinning wheel frequency');
xlabel('Time in sec');
ylabel('Amplitude (a.u)');
title('Reference signals');

% Plot the modulated, demodulated, butterworth low-pass filtered signals in
% time domain
subplot(2,1,2);
plot(time,detector(350,:),'c');
hold on
```

```
plot(time,lock_in_t(350,:),'b');
hold on
plot(time,lock_2in_t(350,:),'r');
hold on
plot(time,lock_in_nt(350,:),'g');
hold on
plot(time,lock_2in_nt(350,:),'k');
legend('Modulated signal at 350th step','LIA1 PSD output at 350th step',
'LIA2 PSD output at 350th step','LIA1 PSD output at 350th step (with noise)',
'Amplitude+noise at 350th step (with noise)',1);
xlabel('Time in sec');
ylabel('Amplitude (a.u)');
title('Signal detected at the 350th step of the delay stage (with and without
gaussian noise)');

% Plot the modulated, demodulated, butterworth low-pass filtered signals in
% frequency domain (without Gaussian noise)
graph3 = figure(3);

subplot(2,1,1);
plot(frequency,abs(detector_fft_t(350,:)),'c');
hold on
pause;
plot(frequency,abs(lock_in_fft_t(350,:)),'b');
hold on
pause;
plot(frequency,abs(lock_2in_fft_t(350,:)),'r');
hold on
pause;
plot(frequency,abs(butter_origin_fft(350,:)),'g');
hold on
pause;
plot(frequency,abs(butter_2origin_fft(350,:)),'k');
legend('Modulated signal at 350th step','Demodulated output (LIA1) at 350th step ',
'Demodulated output (LIA2) at 350th step',
'Demodulated output after LPF (LIA1) at 350th step',
'Demodulated output after LPF (LIA2) at 350th step',1);
xlabel('Frequency in Hz');
ylabel('Amplitude (a.u)');
title('Before and after butterworth low-pass filter at 350th step of the
delay stage');
```

```
% Plot the modulated, demodulated, butterworth low-pass filtered signals in
% frequency domain (with Gaussian noise)
subplot(2,1,2)
plot(frequency,abs(detector_fft_nt(350,:)),'c');
pause;
hold on
plot(frequency,abs(lock_in_fft_nt(350,:)),'b');
pause;
hold on
plot(frequency,abs(lock_2in_fft_nt(350,:)),'r');
pause
hold on
plot(frequency,abs(butter_gaussian_fft(350,:)),'g');
pause
hold on
plot(frequency,abs(butter_2gaussian_fft(350,:)),'k');
legend('Modulated signal at 350th step','Demodulated output (LIA1) at 350th step',
'Demodulated output (LIA2) at 350th step',
'Demodulated output after LPF (LIA1) at 350th step',
'Demodulated output after LPF (LIA2) at 350th step',1);
xlabel('Frequency in Hz');
ylabel('Amplitude (a.u)');
title('Before and after butterworth low-pass filter at 350th step of the
delay stage with gaussian noise');
pause

% Plot the original mean and amplitude signals and compare it the signals
% recovered after filtering process
graph4 = figure(4);
plot(time,reference_amplitude1,'b')
hold on
plot(time,reference_amplitude2,'k')
hold on
plot(time,y,'r');
hold on
plot(time,h,'g');
legend('Original mean','Original amplitude','Recovered mean','Recovered
amplitude');
xlabel('Time in sec');
ylabel('Amplitude (a.u)');
```

Bibliography

ABBOTT-D., AND ZHANG-X.-C. (2007). Scanning the issue: T-ray imaging, sensing, and retection, *Proceedings of the IEEE*, **95**(8), pp. 1509 – 1513.

AL-RAMADIN-Y. (2000). Optical properties of poly(vinyl chloride)/poly(ethylene oxide) blend, *Optical Materials*, **14**(4), pp. 287 – 290.

ANTHONY-H. D. (1960). *Sir Isaac Newton*, Abelard-Schuman Limited.

ARIKAWA-T., NAGAI-M., AND TANAKA-K. (2008). Characterizing hydration state in solution using terahertz time-domain attenuated total reflection spectroscopy, *Chemical Physics Letters*, **457**(1-3), pp. 12 – 17.

ASAKI-M., REDONDO-A., ZAWODZINSKI-T., AND TAYLOR-A. (2002). Dielectric relaxation of electrolyte solutions using terahertz transmission spectroscopy, *Journal of Chemical Physics*, **116**(19), pp. 8469 – 8482.

AUSTON-D., CHEUNG-K., AND SMITH-P. (1984). Picosecond photoconducting Hertzian dipoles, *Applied Physics Letters*, **45**(3), pp. 284 – 286.

AUSTON-D. H. (1988). *Topics in Applied Physics: Ultrafast Optoelectronics*, Springer - Verlag.

AUSTON-D. H., AND NUSS-M. C. (1988). Electrooptic generation and detection of femtosecond electrical transients, *IEEE Journal of Quantum Electronics*, **24**(2), pp. 184 – 197.

BAIRD-D., HUGHES-R. I. G., AND NORNMANN-A. (1998). *Heinrich Hertz: Classical Physicist, Modern Philosopher*, Kluwer Academic Publishers.

BAKER-C., LO-T., TRIBE-W., COLE-B., HOGBIN-M., AND KEMP-M. (2007). Detection of concealed explosives at a distance using terahertz technology, *Proceedings of the IEEE*, **95**(8), pp. 1559 – 1565.

BALAKRISHNAN-J., FISCHER-B. M., MICKAN-S., AND ABBOTT-D. (2006). Novel T-ray liquid spectroscopy via double-modulated differential time-domain spectroscopy, *Proceedings IRMMW-THz*, Shanghai, China, DOI: 10.1109/ICIMW.2006.368654.

BALAKRISHNAN-J., FISCHER-B. M., AND ABBOTT-D. (2008). Double-modulated DTDS-THz liquid spectroscopy using a novel spinning wheel technique, *Proceedings IRMMW-THz*, California, USA, DOI: 10.1109/ICIMW.2008.4665816.

BALAKRISHNAN-J., FISCHER-B. M., AND ABBOTT-D. (2009a). Fixed dual-thickness terahertz liquid spectroscopy using a spinning sample technique, *IEEE Photonics Journal*, **1**(2), pp. 88 – 98.

BALAKRISHNAN-J., FISCHER-B. M., AND ABBOTT-D. (2009b). Sensing the hygroscopicity of polymer and copolymer materials using terahertz time-domain spectroscopy (THz-TDS), *Applied Optics*, **48**(13), pp. 2262 – 2266.

BALAKRISHNAN-J., FISCHER-B. M., AND ABBOTT-D. (2010). Low noise spinning wheel technique for THz material parameter extraction, *Optics Communications*, DOI: 10.1016/j.optcom.2010.01.042.

BAND-Y. B. (2006). *Light and Matter, Electromagnetism, Optics, Spectroscopy, and Lasers*, John Wiley & Sons, Ltd.

BEESON-S., AND MAYER-J. W. (2008). *Patterns of Light: Chasing the Spectrum from Aristotle to LEDs*, Springer.

BERG-H. (2008). Johann Wilhelm Ritter – The Founder of Scientific Electrochemistry, *Review of Polarography*, **54**(2), pp. 99 – 103.

BERSHTEIN-V. A., AND RYZHOV-V. A. (1994). *Advances in Polymer Science*, Vol. 114, Springer-Verlag.

BRITTAIN-E. F. H., GEORGE-W. O., AND WELLS-C. H. J. (1970). *Introduction to Molecular Spectroscopy Theory and Experiment*, Academic Press Inc. (London) Ltd.

BYRANT-J. H. (1998). *Heinrich Hertz's Experiments and Experimental Appratus: His Discovery of Radiowaves and His Delineation of Their Properties*, Kluwer Academic Publishers.

CHANTRY-G., FLEMING-J., NICOL-E. A., WILLIS-H., CUDBY-M., AND BOERIO-F. (1974). Far infra-red spectrum of crystalline polytetrafluoroethylene, *Polymer*, **15**(2), pp. 69 – 73.

CHANTRY-G. W. (1971). *Submillimetre Spectroscopy*, Academic Press, London and New York.

CHENG-L., HAYASHI-S., DOBROIU-A., OTANI-C., KAWASE-K., MIYAZAWA-T., AND OGAWA-Y. (2008). Terahertz-wave absorption in liquids measured using the evanescent field of a silicon waveguide, *Applied Physics Letters*.

CHEREMISINOFF-N. P. (1989). *Handbook of Polymer Science and Technology: Synthesis and properties*, Marcel Dekker, Inc.

DEBYE-P. (1942). Reaction rates in ionic solutions, *Electrochemical Society – Transactions*, **82**, pp. 265 – 271.

DOBROIU-A., SASAKI-Y., SHIBUYA-T., OTANI-C., AND KAWASE-K. (2007). THz-wave spectroscopy applied to the detection of illicit drugs in mail, *Proceedings of the IEEE*, **95**(8), pp. 1566 – 1575.

DUNLOP-J., AND SMITH-G. D. (1994). *Telecommunications Engineering*, CRC Press.

DUTTA-P., AND HORN-P. M. (1981). Low-frequency fluctuations in solids: $1/f$ noise, *Rev. Mod. Phys.*, **53**(3), pp. 497 – 516.

DUTTA-P., AND TOMINAGA-K. (2009). Obtaining low-frequency spectra of acetone dissolved in cyclohexane by terahertz time-domain spectroscopy, *Journal of Physical Chemistry A*, **113**(29), pp. 8235 – 8242.

DUVILLARET-L., GARET-F., AND COUTAZ-J.-L. (1996). Reliable method for extraction of material parameters in terahertz time-domain spectroscopy, *IEEE Journal on Selected Topics in Quantum Electronics*, **2**(3), pp. 739 – 746.

DUVILLARET-L., GARET-F., AND COUTAZ-J.-L. (1999). Noise analysis in THz time-domain spectrosocpy and accuracy enhancement of optical constant determination, *Proceedings of the SPIE - Terahertz Spectroscopy and Applications*, **3617**, pp. 38 – 48.

DUVILLARET-L., GARET-F., ROUX-J.-F., AND COUTAZ-J.-L. (2001). Analytical modeling and optimization of terahertz time-domain spectroscopy experiments using photoswitches as antennas, *IEEE Journal on Selected Topics in Quantum Electronics*, **7**(4), pp. 615 – 623.

EBEWELE-R. O. (1996). *Polymer Science and Technology*, CRC Press.

EBNESAJJAD-S. (2003). *Melt Processible Fluoropolymers: The Definitive User's Guide and Databook*, Plastics Design Library.

ELIZABETH-C. (2007). Röntgen's ray; A story of Wilhelm Konrad Röntgen's discovery of a light that was never on land or sea ([19 –]), Web. http://www.archive.org/details/roentgensraystor00coleuoft.

FEDERICI-J. F., SCHILKIN-B., HUANG-F., GARY-D., BARAT-R., OLIVEIRA-F., AND ZIMDARS-D. (2005). THz imaging and sensing for security applications-explosives, weapons and drugs, *Semiconductor Science and Technology*, **20**, pp. S266 – S280.

FISCHER-B., HELM-H., AND JEPSEN-P. (2007). Chemical recognition with broadband THz spectroscopy, *Proceedings of the IEEE*, **95**(8), pp. 1592 – 1604.

FISCHER-B., HOFFMAN-M., HELM-H., MODJESCH-G., AND JEPSEN-P. U. (2005a). Chemical recognition in terahertz time-domain spectroscopy and imaging, *Semiconductor Science and Technology*, **20**, pp. S246–S253.

FISCHER-B. M. (2005). *Broadband THz Time-Domain Spectroscopy of Biomolecules: A Comprehensive Study of The Dielectric Properties of Biomolecules in the Far-Infrared*, PhD thesis.

FISCHER-B. M., HOFFMANN-M., HELM-H., WILK-R., RUTZ-F., KLEINE-OSTMANN-T., KOCH-M., AND JEPSEN-P. U. (2005b). Terahertz time-domain spectroscopy and imaging of artificial RNA, *Optics Express*, **13**(14), pp. 5205 – 5215.

FISCHER-B. M., HOFFMANN-M., JEPSEN-P. U., AND WALTHER-M. (2005c). Use of the plastic materials topas and zeonex for biotechnological applications in the terahertz range.

FLANDERS-B., CHEVILLE-R., GRISCHKOWSKY-D., AND SCHERER-N. (1996). Pulsed terahertz transmission spectroscopy of liquid $CHCl_3$, CCl_4, and their mixtures, *Journal of physical chemistry*, **100**(29), pp. 11824 – 11835.

FOLTYNOWICZ-R. J., WANKE-M. C., AND MANGAN-M. A. (2005). Atmospheric propagation of THz radiation, *Technical Report*, Sandia National Laboratories.

FRIEDBERG-E. C. (1997). *Correcting the Blueprint of Life: An historical account of the discovery of DNA repair mechanisms*, NY: Cold Spring Harbor Laboratory Press.

FULLER-A. J. B. (1979). *An Introduction to Microwave Theory and Techniques*, Pergamon Press.

GEDDE-U. W. (1999). *Polymer Physics*, Kluwer Academic Publishers.

GERWARD-L. (1999). Paul Villard and his discovery of gamma rays, *Physics in Perspective*, **1**, pp. 367 – 383.

GLOBUS-T., WOOLARD-D., CROWE-T. W., KHROMOVA-T., GELMONT-B., AND HESLER-J. (2006). Terahertz Fourier transform characterization of biological materials in a liquid phase, *Journal of Physics D: Applied Physics*, **39**(15), pp. 3405 – 3413.

GORENFLO-S., TAUER-U., HINKOV-I., LAMBRECHT-A., BUCHNER-R., AND HELM-H. (2006). Dielectric properties of oil-water complexes using terahertz transmission spectroscopy, *Chemical Physics Letters*, **421**(4-6), pp. 494 – 498.

HDPE (2009). Web. http://www.dynalabcorp.com/technical_info_hd_polyethylene.asp.

HERSCHEL (2000). Web. http://www.ipac.caltech.edu/Outreach/Edu/Herschel/herschel.html.

HIRORI-H., YAMASHITA-K., NAGAI-M., AND TANAKA-K. (2004). Attenuated total reflection spectroscopy in time-domain using terahertz coherent pulses, *Japanese Journal of Applied Physics, Part 2: Letters*, **43**(10 A), pp. L1287 – L1289.

HOFFMANN-M. (2006). *Novel Techniques in THz-Time-Domain-Spectroscopy: A Comprehensive Study of the Technical Improvements to THz-TDS*, PhD thesis.

HO-L., MULLER-R., ROMER-M., GORDON-K., HEINAMAKI-J., KLEINEBUDDE-P., PEPPER-M., RADES-T., SHEN-Y., STRACHAN-C., TADAY-P., AND ZEITLER-J. (2007). Analysis of sustained-release tablet film coats using terahertz pulsed imaging, *Journal of Controlled Release*, **119**(3), pp. 253 – 261.

HOUSECROFT-C. E., AND CONSTABLE-E. C. (2006). *Chemistry*, PEARSON Prentice Hall.

HU-B. B., AND NUSS-M. C. (1995). Imaging with terahertz waves, *Optics Letters*, **20**, pp. 1716–1718.

IKEDA-T., MATSUSHITA-A., TATSUNO-M., MINAMI-Y., YAMAGUCHI-M., YAMAMOTO-K., TANI-M., AND HANGYO-M. (2005). Investigation of inflammable liquids by terahertz spectroscopy, *Applied Physics Letters*, **87**(3), art.no. 034105.

IWASZCZUK-K., COOKE-D. G., FUJIWARA-M., HASHIMOTO-H., AND JEPSEN-P. U. (2009). Simultaneous reference and differential waveform acquisition in time-resolved terahertz spectroscopy, *Optics Express*, **17**(24), pp. 21969 – 21976.

JEPSEN-P. U., JENSEN-J. K., AND MOLLER-U. (2008). Characterization of aqueous alcohol solutions in bottles with THz reflection spectroscopy, *Optics Express*, **16**(13), pp. 9318 – 9331.

JEPSEN-P. U., MLLER-U., AND MERBOLD-H. (2007). Investigation of aqueous alcohol and sugar solutions with reflection terahertz time-domain spectroscopy, *Optics Express*, **15**(22), pp. 14717 – 14737.

JIANG-Z., LI-M., AND ZHANG-X.-C. (2000). Dielectric constant measurement of thin films by differential time-domain spectroscopy, *Applied Physics Letters*, **76**(22), pp. 3221 – 3223.

JIN-Y.-S., JEON-S.-G., KIM-G.-J., KIM-J.-I., AND SHON-C.-H. (2007). Fast scanning of a pulsed terahertz signal using an oscillating optical delay line, *Review of Scientific Instruments*, **78**(2), art. no. 023101.

JIN-Y.-S., KIM-G.-J., AND JEON-S.-G. (2006). Terahertz dielectric properties of polymers, *Journal of the Korean Physical Society*, **49**(2), pp. 513 – 517.

KAWASE-K., OGAWA-Y., WATANABE-Y., AND INOUE-H. (2003). Non-destructive terahertz imaging of illicit drugs using spectral fingerprints, *Optics Express*, **11**(20), pp. 2549 – 2554.

KEIDING-S. (1997). Dipole correlation functions in liquid benzenes measured with terahertz time domain spectroscopy, *Journal of Physical Chemistry A*, **101**(29), pp. 5250 – 5254.

KEMP-M. C., TADAY-P. F., COLE-B. E., CLUFF-J. A., FITZGERALD-A. J., AND TRIBE-W. R. (2003). Security applications of terahertz technology, *Proceedings of SPIE - The International Society for Optical Engineering*, **5070**, pp. 44 – 52.

KHANARIAN-G., AND CELANESE-H. (2001). Optical properties of cyclic olefin copolymers, *Optical Engineering*, **40**(6), pp. 1024 – 1029.

KIM-G.-J., JEON-S.-G., KIM-J.-I., AND JIN-Y.-S. (2008). High speed scanning of terahertz pulse by a rotary optical delay line, *Review of Scientific Instruments*, **79**(10), art. no. 106102.

KINDT-J. T., AND SCHMUTTENMAER-C. A. (1996). Far-infrared dielectric properties of polar liquids probed by femtosecond terahertz pulse spectroscopy, *The Journal of Physical Chemistry*, **100**(24), pp. 10373 – 10379.

KLÖPFFER-W. (1984). *Introduction to Polymer Spectroscopy*, Spinger-Verlag.

KNOBLOCH-P., SCHILDNECHT-C., KLEINE-OSTMANN-T., KOCH-M., HOFFMANN-S., HOFMANN-M., REHBERG-E., SPERLING-M., DONHUIJSEN-K., HEIN-G., AND PIERZ-K. (2002). Medical THz imaging: An investigation of histo-pathological samples, *Physics in Medicine and Biology*, **47**(21), pp. 3875 – 3884.

L'ANNUNZIATA-M. F. (2007). *Radioactivity: Introduction and History*, Elsevier Science.

LEE-K.-S., LU-T.-M., AND ZHANG-X.-C. (2003). The measurement of the dielectric and optical properties of nano thin films by THz differential time-domain spectroscopy, *Microelectronics Journal*, **34**(1), pp. 63 – 69.

LEE-Y.-S. (2009). *Principles of Terahertz Science and Technology*, Springer.

LIBBRECHT-K. G., BLACK-E. D., AND HIRATA-C. M. (2003). A basic lock-in amplifier experiment for the undergraduate laboratory, *American Journal of Physics*, **71**(11), pp. 1208 – 1213.

LIU-H.-B., ZHONG-H., KARPOWICZ-N., CHEN-Y., AND ZHANG-X.-C. (2007). Terahertz spectroscopy and imaging for defense and security applications, *Proceedings of the IEEE*, **95**(8), pp. 1514 – 1527.

LUCIA-F. C. D. (2003). *Spectroscopy in the Terahertz Spectral Region*, Springer.

MAIMAN-T. (2000). *Laser Odyssey*, Laser Press.

VAN EXTER-M. P., FATTINGER-CH., AND GRISCHKOWSKY-D. (1989). Terahertz time-domain spectroscopy of water vapor, *Optics Letters*, **14**(20), pp. 1128 – 1130.

MICKAN-S., DORDICK-J., MUNCH-J., ABBOTT-D., AND ZHANG-X.-C. (2002a). Terahertz spectroscopy of bound water in nano suspensions, , **4937**, pp. 49 – 61.

MICKAN-S. P. (2003). *T-ray Biosensing*, PhD thesis.

MICKAN-S. P., LEE-K.-S., LU-T.-M., MUNCH-J., ABBOTT-D., AND ZHANG-X.-C. (2002b). Double modulated differential THz-TDS for thin film dielectric characterization, *Microelectronics Journal*, **33**(12), pp. 1033 – 1042.

MICKAN-S. P., MENIKH-A., LIU-H., MANNELLA-C. A., MACCOLL-R., ABBOTT-D., MUNCH-J., AND ZHANG-X.-C. (2002c). Label-free bioaffinity detection using terahertz technology, *Physics in Medicine and Biology*, **47**(21), pp. 3789 – 3795.

MICKAN-S. P., SHVARTSMAN-R., MUNCH-J., ZHANG-X.-C., AND ABBOTT-D. (2004). Low noise laser-based T-ray spectroscopy of liquids using double-modulated differential time-domain spectroscopy, *Journal of Optics B: Quantum and Semiclassical Optics*, **6**(8), pp. S786 – S795.

MOELLER-L., FEDERICI-J., SINYUKOV-A., XIE-C., LIM-H. C., AND GILES-R. C. (2008). Data encoding on terahertz signals for communication and sensing, *Optics Letters*, **33**(4), pp. 393 –395.

NAFTALY-M., AND DUDLEY-R. (2009). THz spectroscopy for measurement of humidity and moisture.

NAFTALY-M., AND MILES-R. E. (2007). *Terahertz Beam Interactions with Amorphous Materials*, Springer, Netherlands.

NAGAI-N., AND FUKASAWA-R. (2004). Abnormal dispersion of polymer films in the THz frequency region, *Chemical Physics Letters*, **388**, pp. 479 – 482.

OBRADOVIC-J., COLLINS-J. H., HIRSCH-O., MANTLE-M. D., JOHNS-M. L., AND GLADDEN-L. F. (2007). The use of THz time-domain reflection measurements to investigate solvent diffusion in polymers, *Polymer*, **48**(12), pp. 3494 – 3503.

OKA-A., AND TOMINAGA-K. (2006). Terahertz spectroscopy of polar solute molecules in non-polar solvents, *Journal of Non-Crystalline Solids*, **352**(42-49 SPEC. ISS.), pp. 4606 – 4609.

PARK-S.-G., MELLOCH-M. R., AND WEINER-A. M. (1999). Analysis of terahertz waveforms measured by photoconductive and electrooptic sampling, *IEEE Journal of Quantum Electronics*, **35**(5), pp. 810 – 819.

PEDERSEN-J., AND KEIDING-S. (1992). THz time-domain spectroscopy of nonpolar liquids, *IEEE Journal of Quantum Electronics*, **28**(10), pp. 2518 – 2522.

PERKINELMER-INSTRUMENTS. (2000). Low level optical detection using lock-in amplifier techniques, *Technical Report*.

PETONG-P., POTTEL-R., AND KAATZE-U. (2000). Water-ethanol mixtures at different compositions and temperatures. a dielectric relaxation study, *Journal of Physical Chemistry A*, **104**(32), pp. 7420 – 7428.

PIAO-Z., TANI-M., AND SAKAI-K. (1999). Carrier dynamics and thz radiation in biased semiconductor structures, *Proceedings of SPIE - The International Society for Optical Engineering*, **3617**, pp. 49 – 56.

PIESIEWICZ-R., JANSEN-C., WIETZKE-S., MITTLEMAN-D., KOCH-M., AND KURNER-T. (2007a). Properties of building and plastic materials in the THz range, *International Journal of Infrared and Millimeter Waves*, **28**(5), pp. 363 – 371.

PIESIEWICZ-R., KLEINE-OSTMANN-T., KRUMBHOLZ-N., MITTLEMAN-D., KOCH-M., SCHOEBEL-J., AND KUERNER-T. (2007b). Short-range ultra-broadband terahertz communications: Concepts and perspectives, *IEEE Antennas and Propagation Magazine*, **49**(6), pp. 24 – 39.

PNG-G., CHOI-J., NG-B.-H., MICKAN-S., ABBOTT-D., AND ZHANG-X.-C. (2008). The impact of hydration changes in fresh bio-tissue on THz spectroscopic measurements, *Physics in Medicine and Biology*, **53**(13), pp. 3501 – 3517.

PODZOROV-A., AND GALLOT-G. (2008). Low-loss polymers for terahertz applications, *Applied Optics*, **47**(18), pp. 3254–3257.

Polyplastics (2009). Web. http://www.polyplastics.com/Gidb/TopSelectBrandAction.do?brandSelected =6.1&_LOCALE=ENGLISH.

POPPE-A., XU-L., KRAUSZ-F., AND SPIELMANN-C. (1998). Noise characterization of sub-10-fs Ti:sapphire oscillators, *IEEE Journal of Selected Topics in Quantum Electronics*, **4**(2), pp. 179 – 184.

PTFE (2009). Web. http://www.dynalabcorp.com/technical_info_ptfe.asp.

RØNNE-C., THRANE-L., ASTRAND-P.-O., WALLQVIST-A., MIKKELSEN-K. V., AND KEIDING-S. R. (1997). Investigation of the temperature dependence of dielectric relaxation in liquid water by THz reflection spectroscopy and molecular dynamics simulation, *Journal of Chemical Physics*, **107**(14), pp. 5319 – 5331.

SAMMON-C., MURA-C., YARWOOD-J., EVERALL-N., SWART-R., AND HODGE-D. (1998). FTIR-ATR studies of the structure and dynamics of water molecules in polymeric matrixes: A comparison of PET and PVC, *Journal of Physical Chemistry B*, **102**(18), pp. 3402 – 3411.

SATO-T., AND BUCHNER-R. (2005). Cooperative and molecular dynamics of alcohol/water mixtures: The view of dielectric spectroscopy, *Journal of Molecular Liquids*, **117**(1-3), pp. 23 – 31.

SENGUPTA-A., BANDYOPADHYAY-A., BOWDEN-B., HARRINGTON-J., AND FEDERICI-J. (2006). Characterisation of olefin copolymers using terahertz spectroscopy, *Electronics Letters*, **42**(25), pp. 1477 – 1479.

SHEN-Y. C., LO-T., TADAY-P. F., COLE-B. E., TRIBE-W. R., AND KEMP-M. C. (2005). Detection and identification of explosives using terahertz pulsed spectroscopic imaging, *Applied Physics Letters*, **86**, art.no. 241116.

SHIN-J. Y., PARK-J. Y., CHENYANG LIU-J. H., AND KIM-S. C. (2005). Chemical structure and physical properties of cyclic olefin copolymers, *Pure and Applied Chemistry*, **77**(5), pp. 801 – 814.

SIMON-L. (2004). *DARK LIGHT: Electricity and Anxiety from the Telegraph to the X-ray*, Harcourt Inc.

SINYUKOV-A. M., LIU-Z., HOR-Y. L., SU-K., BARAT-R. B., GARY-D. E., MICHALOPOULOU-Z.-H., ZORYCH-I., FEDERICI-J. F., AND ZIMDARS-D. (2008). Rapid-phase modulation of terahertz radiation for high-speed terahertz imaging and spectroscopy, *Optics Letters*, **33**(14), pp. 1593 – 1595.

SMITH-P. R., AUSTON-D. H., AND NUSS-M. C. (1988). Subpicosecond photoconducting dipole antennas., *IEEE Journal of Quantum Electronics*, **24**(2), pp. 255 – 260.

SON-J., RUDD-J. V., AND WHITAKER-J. F. (1992). Noise characterization of a self-mode-locked Ti:sapphire laser, *Optics Letters*, **17**(10), pp. 733 – 735.

SPIRO-I. J., AND SCHLESSINGER-M. (1989). *Infrared Technology Fundamentals*, Marcel Dekker, Inc.

Standard Test Method for Water Absorption of Plastics (1986). *Annual Book of American Society for Testing and Materials*, **8.01**, pp. 532 – 533.

STANFORD-RESEARCH-SYSTEMS. (1999). Model SR830 DSP lock-in amplifier, *Technical Report*.

STAUDINGER-H. (2003). Web. http://www2.chemistry.msu.edu/Portraits/PortraitsHH_Detail.asp?HH_Lname=Staudinger.

TE-C. C., FERGUSON-B., AND ABBOTT-D. (2002). Investigation of biomaterial classification using T-rays, *Proceedings of SPIE - The International Society for Optical Engineering*, **4937**, pp. 294 – 306.

TEEGARDEN-D. M. (2004). *Polymer Chemistry: Introduction to an Indispensable Science*, NSTA Press.

THRANE-L., JACOBSEN-R. H., UHD JEPSEN-P., AND KEIDING-S. R. (1995). THz reflection spectroscopy of liquid water, *Chemical Physics Letters*, **240**(4), pp. 330 – 330.

UNG-B.,BALAKRISHNAN-J., FISCHER-B. M., NG-B. W.-H. AND ABBOTT-D. (2007). Terahertz detection of substances for security related purposes, *Proceedings of SPIE, Smart Structures, Devices, and Systems III*, Adelaide, Australia, **6414**, art. no. 64140V.

VENABLES-D., AND SCHMUTTENMAER-C. (1998). Far-infrared spectra and associated dynamics in acetonitrile-water mixtures measured with femtosecond thz pulse spectroscopy, *Journal of Chemical Physics*, **108**(12), pp. 4935 – 4944.

VENABLES-D. S., AND SCHMUTTENMAER-C. A. (2000a). Spectroscopy and dynamics of mixtures of water with acetone, acetonitrile, and methanol, *Journal of Chemical Physics*, **113**(24), pp. 11222 – 11236.

VENABLES-D. S., AND SCHMUTTENMAER-C. A. (2000b). Structure and dynamics of nonaqueous mixtures of dipolar liquids. ii. molecular dynamics simulations, *Journal of Chemical Physics*, **113**(8), pp. 3249 – 3260.

WANG-S., FERGUSON-B., ABBOTT-D., AND ZHANG-X.-C. (2003). T-ray imaging and tomography, *Journal of Biological Physics*, **29**, pp. 247–256.

WITHAYACHUMNANKUL-W., FISCHER-B. M., AND ABBOTT-D. (2008). Material thickness optimization for transmission-mode terahertz time-domain spectroscopy, *Optics Express*, **16**(10), pp. 7382 – 7396.

WITHAYACHUMNANKUL-W., PNG-G. M., YIN-X. X., ATAKARAMIANS-S., JONES-I., LIN-H. Y., UNG-B. S. Y., BALAKRISHNAN-J., NG-B. W.-H., FERGUSON-B., MICKAN-S. P., FISCHER-B., AND ABBOTT-D. (2007). T-ray sensing and imaging, *Proceedings of the IEEE*, **95**(8), pp. 1528 – 1558.

WITTCOFF-H, REUBEN-B. G., AND PLOTKIN-J. S. (2004). *Industrial Organic Chemicals*, John Wiley & Sons, Inc.

YASUI-T., AND ARAKI-T. (2005). Dependence of terahertz electric fields on electric bias and modulation frequency in pulsed terahertz emissions from electrically-modulated photoconductive antenna detected with free-space electro-optic sampling, *Japanese Journal of Applied Physics, Part 1: Regular Papers and Short Notes and Review Papers*, **44**(4 A), pp. 1777 – 1780.

YIN-X. (2008). *Pattern Pecognition and Tomographic Reconstruction with Terahertz Signals for Applications in Biomedical Engineering*, PhD thesis.

YU-B., ZENG-F., XING-Q., AND ALFANO-R. (2003). Probing dielectric relaxation properties of liquid cs_2 with terahertz time-domain spectroscopy, *Applied Physics Letters*, **82**(26), pp. 4633 – 4635.

ZHANG-C., AND DURBIN-S. M. (2006). Hydration-induced far-infrared absorption increase in myoglobin, *Journal of Physical Chemistry B*, **110**(46), pp. 23607 – 23613.

Symbols & Glossary

The commonly used acronyms and symbols used in this Thesis is given in the table below. The page numbers for each entry refer to the first use of the symbol or acronym in the text.

Symbols & Acronyms	Description	Page
$\mathbf{H}$	magnetic field	8
$\mathbf{E}$	electric field	8
f	frequency (Hertz)	8
E	photon energy	8
h	Planck's constant (Joules per second)	8
λ	wavelength (m)	8
ASTM D570	standard test method for water absorption of plastics 1986	63
BNC	bayonet neill-concelman	33
COC	cyclic-olefin copolymer	51
CPM	colliding-pulse passively modelocked	22
CFC	chlorofluorocarbon	50
CS_2	carbon disulphide	72
DNA	deoxyribonucleic acid	73
ESR	electron spin resonance	9
EO	electro-optic	22
FTIR	Fourier transform infrared	48
FTIR-ATR	Fourier transform infrared - attenuated total reflectance	63
GaAs	gallium arsenide	2
GPIB	general purpose interface bus	158
HDPE	high density polyethylene	5
IR	infrared	13
LIA1	lock-in amplifier one	95
LIA2	lock-in amplifier two	96
LPF	low pass filter	155

Symbols & Acronyms	Description	Page
MW	megawatt	10
MD	molecular dynamics	73
Mb	myglobin	73
MRI	magnetic resonance imaging	90
NMR	nuclear magnetic resonance	9
ND	neutral density	157
PMMA	poly(methyl methacrylate)	5
PVC	polyvinyl chloride	5
PTFE	polytetrafluoroethylene	5
PC	polycarbonate	58
PCB	printed circuit board	33
PE	polyethylene	73
PET	polyethylene terephthalate	73
PSD	phase sensitive detection	126
SOS	silicon-on-sapphire	2
SC	Subtilisin Carlsberg	73
SNR	signal-to-noise ratio	90
THz	terahertz	2
THz-TDS	terahertz time-domain spectroscopy	4
THz-DTDS	terahertz differential time-domain spectroscopy	4
TCF	analytic time correlation function	73
TIR	total internal reflection	87
TD-ATR	time-domain attenuated total reflection	110
UV	ultraviolet	15

Index

Résumé

Jegathisvaran Balakrishnan was born on March 20, 1982, in Johor, Malaysia and completed his Diploma degree (Merit) in Electronic and Telecommucation Engineering from Ngee Ann Polytechnic, Singapore, in 2003 and graduated from a Bachelor of Engineering degree (Hons) in Electrical & Electronic Engineering at the University of Adelaide, Australia in 2005.

He commenced his PhD in 2006 at the National T-ray Facility, School of Electrical & Electronic Engineering, The University of Adelaide, Australia under the supervision of Prof Derek Abbott and Dr Bernd M. Fischer.

Jegathisvaran has won a number of awards, including the Cisco System Prize (2003), Sarawak Alumni Scholarship (2004-2005), Postgraduate Divisional Scholarship (2006), and the IEEE SA Travel grant (2008). He is a student member of the IEEE South Australia, and The International Society for Optical Engineering (SPIE). He has authored and co-authored 11 peer-reviewed publications.

Scientific Genealogy